PHYSICAL REVIEW D **95,** 074038 (2017)

Influence of confining gluon configurations on the $P \to \gamma^*\gamma$ transition form factors

Sergei N. Nedelko* and Vladimir E. Voronin†

Bogoliubov Laboratory of Theoretical Physics, JINR, 141980 Dubna, Russia

(Received 9 December 2016; published 25 April 2017)

Transition form factors $F_{P\gamma^*\gamma^{(*)}}$ of pseudoscalar mesons are studied within the framework of the domain model of confinement, chiral symmetry breaking, and hadronization. In this model the QCD vacuum is described by the statistical ensemble of domain wall networks which represents the almost everywhere homogeneous Abelian (anti-)self-dual gluon field configurations. Calculations of the form factors are performed consistently with mass spectra of mesons, their weak and strong decay constants. Influence of the nonperturbative intermediate range gluon fields on behavior of pion transition form factor at large Q^2 is of particular interest. It is found that $Q^2F_{\pi\gamma^*\gamma}(Q^2)$ approaches a constant value at asymptotically large Q^2. However, due to the contribution of confining gluon fields this limit exceeds the standard factorization bound, though the form factor complies with Belle data more likely than with *BABAR* ones. At the same time the generally accepted factorization bound is shown to be satisfied for the case of the symmetric kinematics, $Q^2F_{P\gamma^*\gamma^*}(Q^2)$. Peculiarities of description of η, η', and η_c form factors within the model are discussed in detail.

DOI: 10.1103/PhysRevD.95.074038

I. INTRODUCTION

Experimental data for pion transition form factor $F_{\pi\gamma^*\gamma}$ obtained by the *BABAR* Collaboration [1] indicate growth of $Q^2F_{\pi\gamma^*\gamma}$ at large Q^2 that is inconsistent with prediction of QCD factorization theorems [2]

$$F_{\pi\gamma^*\gamma} \sim \frac{\sqrt{2}f_\pi}{3Q^2}\int_0^1 dx\frac{\phi_\pi^{\rm as}(x)}{x} = \frac{\sqrt{2}f_\pi}{Q^2},$$
$$\phi_\pi^{\rm as}(x) = 6x(1-x), \tag{1}$$

where $f_\pi = 131$ MeV, and $\phi_\pi^{\rm as}(x)$ is the asymptotics of pion distribution amplitude at large Q^2. Published later experimental results carried out by the Belle [3] Collaboration demonstrate qualitatively different behavior at large momenta, though they still allow violation of bound (1). These intriguing though so far incomplete experimental results have motivated extensive theoretical investigations of pion electromagnetic transition form factor $F_{\pi\gamma^*\gamma}$ and QCD factorization in exclusive hadronic processes. Transition form factors were considered within the framework of light-cone [4–6] and anomaly sum rules [7,8], local-duality version of QCD sum rules [9], modified perturbative approach based on the k_T factorization theorem [10,11], dispersion relations [12], light-front holographic QCD [13–16], Dyson-Schwinger equations [17], nonlocal chiral quark models [18–21], light-front quark model [22], vector-meson dominance model and its modifications [23,24], within chiral effective theory with resonances [25], instanton liquid model [26], and models involving physics beyond the Standard Model [27]. Contribution of Adler-Bell-Jackiw triangle anomaly to $\pi^0 \to \gamma^*\gamma$ process was investigated in [28].

Disagreement between bound (1) and the *BABAR* data aroused discussion about validity of the latter [4,17]. The findings demonstrate that higher local operator product expansion and α_s corrections to Eq. (1) are too small to describe *BABAR* data, and one should take into account nonlocal or non-OPE contributions [7]. These corrections may originate from nonlocal condensates, instantons, or short strings. Alternatively, growth of $Q^2F_{\pi\gamma^*\gamma}$ at large Q^2 can be described by "flat" (nonvanishing at the endpoints $x = 0$ and $x = 1$) distribution amplitude [29–31].

In this paper we consider behavior of the transition form factors within the approach based on the description of QCD vacuum as statistical ensemble of domain wall networks representing an ensemble of almost everywhere homogeneous Abelian (anti-)self-dual fields, which are characterized by the nonzero gluon condensates, first of all the scalar $\langle g^2F^2\rangle$ and the absolute value of the pseudoscalar $\langle|g^2\tilde{F}F|\rangle = \langle g^2F^2\rangle$ ones. Motivation for this approach as well as details related to the study of static and dynamical confinement, realization of chiral $SU_L(N_f) \times SU_R(N_f)$ and $U_A(1)$ symmetries in terms of quark-gluon as well as colorless hadron degrees of freedom can be found in papers [32–38] and references therein, where also derivation of the effective meson action used in the present paper is described in detail. Relation of the present approach to the methods based on a combination of the Bethe-Salpeter equation with Dyson-Schwinger equations and functional renormalization group and models based on soft wall AdS/QCD approach was discussed in [37]. The effective meson action allows one to compute the mass spectrum, decay,

*nedelko@theor.jinr.ru
†voronin@theor.jinr.ru

and transition constants as well as form factors describing the strong, electromagnetic, and weak interactions of various mesons within the universal for all mesons setup. Parameters of the model are the infrared limits of the renormalized quark masses and strong coupling constant, scalar gluon condensate $\langle\alpha_s F^2\rangle$, and the mean domain size. The latter can be related to topological susceptibility of pure Yang-Mills vacuum. Overall precision of the approach in the description of the wide range of meson phenomenology (masses of light, heavy-light mesons, and heavy quarkonia, leptonic decay constants, transition constants, all of the above including excited mesons) is about 10%–15% with few exceptions. Throughout all calculations the same values of parameters are used as it is supposed by their physical meaning [37]; see Table I.

The main purpose of the present paper is to investigate how the explicit presence of the background domain structured gluon field affects transition form factors of pseudoscalar mesons and strong decay constants of vector mesons g_{VPP}. In this context the most relevant feature of the present approach is the invariance of meson effective action with respect to the local gauge transformations of the background field. The nonlocal meson-quark vertices depend on the covariant derivatives in the presence of a nonperturbative domain structured gluon field. Within the formalism used in this paper, both quark propagators and meson-quark vertices are translation invariant up to a gauge transformation. As a result, energy-momentum is conserved only in the entire diagram describing interaction between mesons, leptons, and photons, but it is not conserved in every meson-quark vertex separately. Averaging of these diagrams over configurations of the nonperturbative field leads to contributions that are absent if just a global gauge invariance is assumed as it is usually done in nonlocal models of hadronization. This is the most relevant to our task feature of the effective meson action, derived within the domain model, as it becomes a source for violation of factorization properties since it may mix up soft and hard parts of the amplitudes, short and large distance subprocesses. It is shown that the background gluon fields, typical for the domain model, do not cause growth of $Q^2F_{\pi\gamma^*\gamma}$ at large Q^2, and calculation of the asymptotic behavior indicates that

$$F_{\pi\gamma^*\gamma} \sim \varkappa_{\gamma^*\gamma}\frac{\sqrt{2}f_\pi}{Q^2}, \qquad \varkappa_{\gamma^*\gamma} = 1.23, \tag{2}$$

so that $Q^2F_{\pi\gamma^*\gamma}$ approaches a constant value at large Q^2 in qualitative agreement with factorization prediction, but the value of constant $\varkappa_{\gamma^*\gamma}$ substantially differs from unity. At the same time, asymptotic behavior of the form factor in symmetric kinematics with two photons with equal virtuality Q^2,

$$F_{\pi\gamma^*\gamma^*} \sim \varkappa_{\gamma^*\gamma^*}\frac{\sqrt{2}f_\pi}{3Q^2}, \qquad \varkappa_{\gamma^*\gamma^*} = 1, \tag{3}$$

calculated within the present model, matches factorization prediction

$$F_{\pi\gamma^*\gamma^*} \sim \frac{\sqrt{2}f_\pi}{3Q^2}\int_0^1 dx\phi_\pi^{\mathrm{as}}(x) = \frac{\sqrt{2}f_\pi}{3Q^2}. \tag{4}$$

Within the present calculation, the deviation of $\varkappa_{\gamma^*\gamma}$ from unity manifestly originates from the nonconservation of the energy-momentum in the quark-meson vertices and quark propagators separately due to interaction of quarks and gluons with the background confining gluon fields. The energy-momentum is conserved only for the whole locally gauge invariant amplitude of the process $\pi \to \gamma^*\gamma^{(*)}$. In the presence of the vacuum gluon fields under consideration the propagators and vertices are translation invariant only up to a gauge transformation of the background gluon fields. Equivalently, in the presence of the long/intermediate range vacuum gluon fields, the locally gauge invariant amplitudes built of the nonperturbative quark propagators and vertices are translation invariant and ensure energy-momentum conservation.

For symmetric kinematics these specific effects are suppressed and do not influence the asymptotic behavior, while they directly contribute to asymptotic behavior of the form factor for asymmetric kinematics. Relation (4) is reproduced much better than (1). This observation looks natural because a straightforward QCD factorization works best of all in the former case, i.e. when both photons are highly virtual [4,39].

It is important for overall consistency of the formalism that analogous terms originating from the local gauge invariance of the physical amplitudes critically affect the strong decays of vector mesons into a couple of pseudoscalar ones. Relaxation of the local color gauge invariance to the global one leads to drastic disagreement between experimental and calculated values of the decay constants g_{VPP}, particularly $g_{\rho\pi\pi}$. In this context, strong underestimation of decay constant $g_{\rho\pi\pi}$ typical for NJL-type models of hadronization [40,41] cannot be attributed just to the oversimplified local character of meson-quark interaction; nonlocality itself is not sufficient for consistent description of masses and strong decay constants. The local color gauge invariance of the nonlocal effective meson-meson interactions mediated by the quark-gluon interactions appears to be of crucial importance.

The paper is organized as follows. Brief review of the effective meson action is given in Sec. II. Details of calculations of form factors are presented in Sec. III. Section IV is devoted to decay constants of vector mesons into a couple of pseudoscalar mesons. Section V contains conclusions and discussion of the unsolved problems. Details of calculations are given in the appendices.

TABLE I. Values of parameters fitted to the mass spectrum [37] and used for calculations in the present paper.

$m_{u/d}$ (MeV)	m_s (MeV)	m_c (MeV)	m_b (MeV)	Λ (MeV)	α_s	R (fm)
145	376	1566	4879	416	3.45	1.12

II. EFFECTIVE MESON ACTION

Details of motivation of the domain model and derivation of the effective action within the domain model have been discussed from different points of view in several papers [35,37]. A short overview of the hadronization procedure is given in Appendix A. The Euclidean functional integral of the domain model with the effective meson action derived by means of the hadronization procedure has the following structure:

$$Z=\mathcal{N}\int D\phi_{\mathcal{Q}}\exp\left\{-\frac{\Lambda^2}{2}\frac{h_{\mathcal{Q}}^2}{g^2C_{\mathcal{Q}}^2}\int d^4x\phi_{\mathcal{Q}}^2(x)-\sum_{k=2}^{\infty}\frac{1}{k}W_k[\phi]\right\}, \tag{5}$$

$$\begin{aligned}
W_k[\phi] &= \sum_{\mathcal{Q}_1\ldots\mathcal{Q}_k} h_{\mathcal{Q}_1}\ldots h_{\mathcal{Q}_k}\int d^4x_1\ldots \\
&\quad\times\int d^4x_k\Phi_{\mathcal{Q}_1}(x_1)\ldots\Phi_{\mathcal{Q}_k}(x_k)\Gamma^{(k)}_{\mathcal{Q}_1\ldots\mathcal{Q}_k}(x_1,\ldots,x_k),\\
\Phi_{\mathcal{Q}}(x) &= \int\frac{d^4p}{(2\pi)^4}e^{ipx}\mathcal{O}_{\mathcal{Q}\mathcal{Q}'}(p)\tilde{\phi}_{\mathcal{Q}'}(p),\\
C_{\mathcal{Q}} &= C_J,\qquad C^2_{S/P}=2C^2_{V/A}=\frac{1}{9},
\end{aligned} \tag{6}$$

where condensed index $\mathcal{Q}\equiv\{aJLn\}$ denotes all meson quantum numbers like spin parity in the ground state $J\in\{S,P,V,A\}$, orbital momentum l contributing to the total angular momentum (spin) for orbital excitations, radial quantum number n, flavor $SU(N)$ multiplets a, and space-time indices. Transformation $\mathcal{O}_{\mathcal{Q}\mathcal{Q}'}$ relates physical meson fields $\phi_{\mathcal{Q}}$ to auxiliary fields $\Phi_{\mathcal{Q}}$ introduced during hadronization. The meson masses $M_{\mathcal{Q}}$ and quark-meson coupling constants $h_{\mathcal{Q}}$ are determined by the quadratic part of the effective meson action *via* equations

$$1=\frac{g^2C_{\mathcal{Q}}^2}{\Lambda^2}\tilde{\Pi}_{\mathcal{Q}}(-M^2_{\mathcal{Q}}|B), \tag{7}$$

$$h_{\mathcal{Q}}^{-2}=\frac{d}{dp^2}\tilde{\Pi}_{\mathcal{Q}}(p^2|B)|_{p^2=-M^2_{\mathcal{Q}}}, \tag{8}$$

where $\bar{\Pi}_{\mathcal{Q}}(p^2|B)$ is two-point correlator $\Gamma_{\mathcal{Q}\mathcal{Q}'}$ diagonalized with respect to all quantum numbers [see Fig. (1) and Eqs. (10) and (11)] and put on mass shell $p^2=-M^2$:

$$\begin{aligned}
&\tilde{\phi}^{\dagger}_{\mathcal{Q}}(-p)[\mathcal{O}^T(p)\tilde{\Gamma}^{(2)}(p)\mathcal{O}(p)]_{\mathcal{Q}\mathcal{Q}'}\tilde{\phi}_{\mathcal{Q}'}(p)|_{p^2=-M^2_{\mathcal{Q}}}\\
&\quad=\tilde{\Pi}_{\mathcal{Q}}(-M^2_{\mathcal{Q}}|B)\tilde{\phi}^{\dagger}_{\mathcal{Q}}(-p)\tilde{\phi}_{\mathcal{Q}}(p)|_{p^2=-M^2_{\mathcal{Q}}}.
\end{aligned} \tag{9}$$

Masses $M_{\mathcal{Q}}$ correspond to the poles of meson propagators, while relation (8) for meson-quark interaction constants $h_{\mathcal{Q}}$ provides correct residue at the pole. This relation is known also as a compositeness condition for meson fields. Integration variables $\phi_{\mathcal{Q}}$ in the functional integral (5) correspond to the physical meson fields that diagonalize the quadratic part of the effective meson action (6) in momentum representation, which is achieved by means of transformation $\mathcal{O}(p)$. Effective action (6) is expressed in terms of colorless composite fields $\Phi_{\mathcal{Q}}$ related to the physical meson fields through the transformation $\mathcal{O}(p)$,

$$\tilde{\Phi}_{\mathcal{Q}}(p)=\mathcal{O}_{\mathcal{Q}\mathcal{Q}'}(p)\tilde{\phi}_{\mathcal{Q}'}(p),$$

and k-point nonlocal vertex functions $\Gamma^{(k)}_{\mathcal{Q}_1\ldots\mathcal{Q}_k}$:

$$\begin{aligned}
\Gamma^{(2)}_{\mathcal{Q}_1\mathcal{Q}_2} &= \overline{G^{(2)}_{\mathcal{Q}_1\mathcal{Q}_2}(x_1,x_2)}-\Xi_2(x_1-x_2)\overline{G^{(1)}_{\mathcal{Q}_1}G^{(1)}_{\mathcal{Q}_2}},\\
\Gamma^{(3)}_{\mathcal{Q}_1\mathcal{Q}_2\mathcal{Q}_3} &= \overline{G^{(3)}_{\mathcal{Q}_1\mathcal{Q}_2\mathcal{Q}_3}(x_1,x_2,x_3)}-\frac{3}{2}\Xi_2(x_1-x_3)\overline{G^{(2)}_{\mathcal{Q}_1\mathcal{Q}_2}(x_1,x_2)G^{(1)}_{\mathcal{Q}_3}(x_3)}\\
&\quad+\frac{1}{2}\Xi_3(x_1,x_2,x_3)\overline{G^{(1)}_{\mathcal{Q}_1}(x_1)G^{(1)}_{\mathcal{Q}_2}(x_2)G^{(1)}_{\mathcal{Q}_3}(x_3)},\\
\Gamma^{(4)}_{\mathcal{Q}_1\mathcal{Q}_2\mathcal{Q}_3\mathcal{Q}_4} &= \overline{G^{(4)}_{\mathcal{Q}_1\mathcal{Q}_2\mathcal{Q}_3\mathcal{Q}_4}(x_1,x_2,x_3,x_4)}-\frac{4}{3}\Xi_2(x_1-x_2)\overline{G^{(1)}_{\mathcal{Q}_1}(x_1)G^{(3)}_{\mathcal{Q}_2\mathcal{Q}_3\mathcal{Q}_4}(x_2,x_3,x_4)}\\
&\quad-\frac{1}{2}\Xi_2(x_1-x_3)\overline{G^{(2)}_{\mathcal{Q}_1\mathcal{Q}_2}(x_1,x_2)G^{(2)}_{\mathcal{Q}_3\mathcal{Q}_4}(x_3,x_4)}+\Xi_3(x_1,x_2,x_3)\overline{G^{(1)}_{\mathcal{Q}_1}(x_1)G^{(1)}_{\mathcal{Q}_2}(x_2)G^{(2)}_{\mathcal{Q}_3\mathcal{Q}_4}(x_3,x_4)}\\
&\quad-\frac{1}{6}\Xi_4(x_1,x_2,x_3,x_4)\overline{G^{(1)}_{\mathcal{Q}_1}(x_1)G^{(1)}_{\mathcal{Q}_2}(x_2)G^{(1)}_{\mathcal{Q}_3}(x_3)G^{(1)}_{\mathcal{Q}_4}(x_4)}.
\end{aligned} \tag{10}$$

The vertices $\Gamma^{(n)}$ are expressed *via* quark loops $G^{(l)}_{\mathcal{Q}_1\ldots\mathcal{Q}_k}$ averaged over the background field

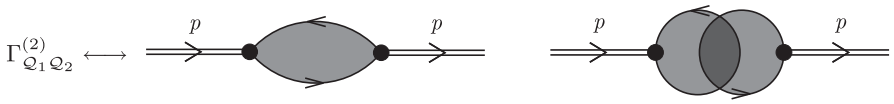

FIG. 1. Diagrams contributing to the equation for the meson masses (7) and quark-meson coupling constants (8). Light gray color denotes averaging over configurations of the domain bulk background field. Dark gray color denotes correlation of the quark loops directly due to the finite range correlators in the domain ensemble. The two-loop diagram is particularly important for the masses of η and η'.

$$\begin{aligned}\overline{G^{(k)}_{\mathcal{Q}_1\ldots\mathcal{Q}_k}(x_1,\ldots,x_k)} &= \int d\sigma_B \mathrm{Tr} V_{\mathcal{Q}_1}(x_1|B)S(x_1,x_2|B)\ldots V_{\mathcal{Q}_k}(x_k|B)S(x_k,x_1|B),\\ &\times\ \overline{G^{(l)}_{\mathcal{Q}_1\ldots\mathcal{Q}_l}(x_1,\ldots,x_l)G^{(k)}_{\mathcal{Q}_{l+1}\ldots\mathcal{Q}_k}(x_{l+1},\ldots,x_k)}\\ &= \int d\sigma_B \mathrm{Tr}\{V_{\mathcal{Q}_1}(x_1|B)S(x_1,x_2|B)\ldots V_{\mathcal{Q}_k}(x_l|B)S(x_l,x_1|B)\}\\ &\times \mathrm{Tr}\{V_{\mathcal{Q}_{l+1}}(x_{l+1}|B)S(x_{l+1},x_{l+2}|B)\ldots V_{\mathcal{Q}_k}(x_k|B)S(x_k,x_{l+1}|B)\},\end{aligned} \tag{11}$$

where the bar denotes averaging over all configurations of the background gluon field with measure $d\sigma_B$; see [34,35]. There are two types of contributions to vertex functions $\Gamma^{(k)}$—one-loop diagrams and $n \le k$-loop diagrams connected by the correlators of the statistical ensemble of the nonperturbative background fields—almost everywhere homogeneous (anti-)self-dual Abelian gluon fields.

A simplified version of the domain model which allows one to compute the effective action analytically is based on two main approximations. Quark and gluon propagators are computed in the homogeneous background field, which represents the domain bulk, while the finite size of domains is neglected at this step. The finite mean size is taken into account through the domain ensemble correlators $\Xi_n(x_1,\ldots,x_n)$ which have geometrical interpretation in terms of a volume of overlap of n four-dimensional hyperspheres with radius R and centers at the points $x_1,\ldots,x_k$ according to the formalism derived in [34,35]. As it has already been mentioned, meson vertices $\Gamma^{(k)}_{\mathcal{Q}_1\ldots\mathcal{Q}_k}$ are averaged over all configurations of the homogeneous (anti-)self-dual Abelian gluon fields: (anti-)self-duality, color, and space-time orientation. The latter is achieved by means of generating formula

$$\begin{aligned}\langle \exp(i f_{\mu\nu}J_{\mu\nu})\rangle &= \frac{\sin\sqrt{2(J_{\mu\nu}J_{\mu\nu} \pm J_{\mu\nu}\tilde{J}_{\mu\nu})}}{\sqrt{2(J_{\mu\nu}J_{\mu\nu} \pm J_{\mu\nu}\tilde{J}_{\mu\nu})}},\\ f_{\alpha\beta} &= \frac{\hat{n}}{2\upsilon\Lambda^2}B_{\alpha\beta}, \quad \upsilon = \mathrm{diag}\left(\frac{1}{6},\frac{1}{6},\frac{1}{3}\right),\end{aligned} \tag{12}$$

where tensor $f_{\mu\nu}$ is related to the strength of the Abelian (anti-)self-dual background field

$$\begin{aligned}&\hat{B}_\mu = -\frac{1}{2}\hat{n}B_{\mu\nu}x_\nu, \quad \hat{n} = t^3\cos\xi + t^8\sin\xi,\\ &\tilde{B}_{\mu\nu} = \frac{1}{2}\epsilon_{\mu\nu\alpha\beta}B_{\alpha\beta} = \pm B_{\mu\nu}, \quad \hat{B}_{\rho\mu}\hat{B}_{\rho\nu} = 4\upsilon^2\Lambda^4\delta_{\mu\nu},\\ &f_{\alpha\beta} = \frac{\hat{n}}{2\upsilon\Lambda^2}B_{\alpha\beta}, \quad \upsilon = \mathrm{diag}\left(\frac{1}{6},\frac{1}{6},\frac{1}{3}\right), \quad f_{\mu\alpha}f_{\nu\alpha} = \delta_{\mu\nu},\end{aligned}$$

and $J_{\mu\nu}$ is an arbitrary antisymmetric tensor. For example, generating formula leads to

$$\langle f_{\mu\nu}\rangle = 0, \langle f_{\mu\nu}f_{\alpha\beta}\rangle = \frac{1}{3}(\delta_{\mu\alpha}\delta_{\nu\beta} - \delta_{\mu\beta}\delta_{\nu\alpha} \pm \varepsilon_{\mu\nu\alpha\beta}).$$

In this approximation vertex $V^{aJln}_{\mu_1\ldots\mu_l}$ is defined by the formulas

$$\begin{aligned}V^{aJln}_{\mu_1\ldots\mu_l} &= \mathcal{C}_{ln}\mathcal{M}^a\Gamma^J F_{nl}\left(\frac{\overleftrightarrow{\mathcal{D}}^2(x)}{\Lambda^2}\right)T^{(l)}_{\mu_1\ldots\mu_l}\left(\frac{1}{i}\frac{\overleftrightarrow{\mathcal{D}}(x)}{\Lambda}\right),\\ \mathcal{C}^2_{ln} &= \frac{l+1}{2^l n!(n+l)!}, \qquad F_{nl}(s) = s^n\int_0^1 dt t^{n+l}\exp(st),\\ \overleftrightarrow{\mathcal{D}}^{ff'}_\mu &= \xi_f\overleftarrow{\mathcal{D}}_\mu - \xi_{f'}\vec{\mathcal{D}}_\mu, \qquad \overleftarrow{\mathcal{D}}_\mu(x) = \overleftarrow{\partial}_\mu + i\hat{B}_\mu(x),\\ \vec{\mathcal{D}}_\mu(x) &= \vec{\partial}_\mu - i\hat{B}_\mu(x),\\ \xi_f &= \frac{m_{f'}}{m_f + m_{f'}}, \qquad \xi_{f'} = \frac{m_f}{m_f + m_{f'}},\end{aligned} \tag{13}$$

where $\mathcal{M}^a$ is the flavor matrix, Γ^J is a Dirac matrix with $J \in \{S,P,V,A\}$, and x is the center of mass of the quarks with flavors f and f' entering and exiting the vertex in (11). The form of the radial part F_{nl} of the vertex is determined by the propagator of the gluon fluctuations charged with respect to the Abelian background. The quark propagator in the presence of the Abelian (anti-)self-dual homogeneous field has the form

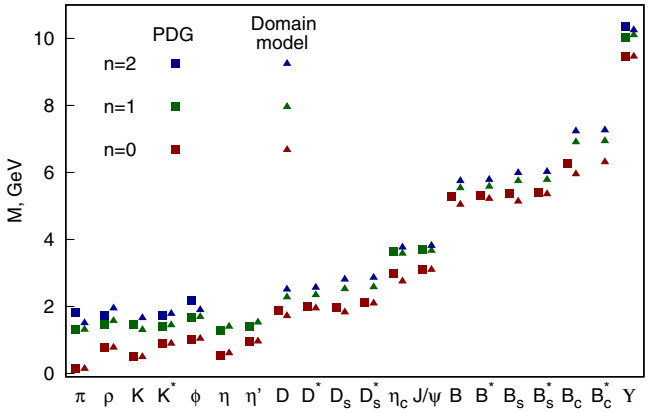

FIG. 2. The masses of various radially excited mesons calculated with the values of parameters shown in Table II.

$$S_f(x,y|B) = \exp\left(-\frac{i}{2}\hat{n}x_\mu B_{\mu\nu}y_\nu\right)H_f(x-y|B),$$

$$\tilde{H}_f(p|B) = \frac{1}{2\upsilon\Lambda^2}\int_0^1 ds e^{(-p^2/2\upsilon\Lambda^2)s}\left(\frac{1-s}{1+s}\right)^{m_f^2/4\upsilon\Lambda^2} \times\left[p_\alpha\gamma_\alpha \pm is\gamma_5\gamma_\alpha f_{\alpha\beta}p_\beta + m_f\left(P_\pm + P_\mp\frac{1+s^2}{1-s^2} - \frac{i}{2}\gamma_\alpha f_{\alpha\beta}\gamma_\beta\frac{s}{1-s^2}\right)\right]. \quad (14)$$

The values of parameters of the model given in Table I were fitted to the masses of ground-state mesons $\pi, \rho, K, K^*, J/\psi, \Upsilon, \eta'$ and were used for calculation of the decay and transition constants as well as masses of a wide range of mesons [37]. The results are illustrated in Fig. 2 and Table II, respectively.

TABLE II. Decay and transition constants of various mesons [37].

Meson	n	$f_P^{\rm exp}$ (MeV)	f_P (MeV)	Meson	n	$g_{V\gamma}^{\rm exp}$ [42]	$g_{V\gamma}$
π	0	130 [42]	140	ρ	0	0.2	0.2
$\pi(1300)$	1		29	ρ	1		0.053
K	0	156 [42]	175	ω	0	0.059	0.067
$K(1460)$	1		27	ω	1		0.018
D	0	205 [42]	212	ϕ	0	0.074	0.071
D	1		51	ϕ	1		0.02
D_s	0	258 [42]	274	J/ψ	0	0.09	0.06
D_s	1		57	J/ψ	1		0.015
B	0	191 [42]	187	Υ	0	0.025	0.014
B	1		55	Υ	1		0.0019
B_s	0	253 [43]	248				
B_s	1		68				
B_c	0	489 [43]	434				
B_c	1		135				

III. TWO-PHOTON DECAY CONSTANTS AND TRANSITION FORM FACTORS

Weak and electromagnetic interactions can be introduced into meson effective action (6) by the standard requirement of the local gauge invariance which generates two types of gauge boson couplings—the standard one with the local quark current and direct interaction with the nonlocal quark-meson vertices. Detailed derivation for the model under consideration can be found in paper [37]. In particular, interaction of the pseudoscalar mesons with two photons in the lowest order over quark-meson coupling constants (or, equivalently, to the lowest order in $1/N_c$) is formally described by four terms represented diagrammatically in Fig. 3, where diagrams C and D include additional meson-quark-photon coupling. However, explicit calculations show that contribution of diagrams C and D vanish. Two other diagrams include the standard local electromagnetic interaction of quarks. Besides the triangle diagram A there can be an additional term B, which directly includes the correlator of the nonperturbative gluon field. The latter term is analogous to the direct instanton contribution considered in paper [26] within the instanton liquid model. A nonzero contribution of diagram B to the form factors of π and η mesons necessarily requires violation of flavor symmetry. This condition is irrelevant to η' and η_c mesons, and one may expect that these mesons are much more sensitive to correlations of the vacuum field ensemble crucial for the two-loop diagram B. We shall return to discussion of this issue after studying the form factors generated by the triangle diagram. Its contribution to the vertex for interaction between the meson $\phi^{aP00}(x)$ and electromagnetic fields $A_\mu(y)$, $A_\nu(z)$ has the form

$$T^{an}_{\mu\nu}(x,y,z) = h_{aP0n}\sum_{n',f}\mathcal{O}^{ab}_{nn'}\mathrm{Tr}\int d\sigma_B e_f^2\mathcal{M}^b_{ff}\mathcal{C}_{n'0}F_{n'0}(x)i\gamma_5 \times S_f(x,y|B)\gamma_\mu S_f(y,z|B)\gamma_\nu S_f(z,x|B). \quad (15)$$

Here f is the flavor index, and Tr denotes trace of the color and Dirac matrices. The index n denotes the radial quantum number. The quark-meson coupling constant h_{aP00} is defined by (8). The coefficients $\mathcal{O}^{ab}_{nn'}$ describe transformation from auxiliary meson fields $\Phi^b_{n'}$ to physical meson fields ϕ^a_n and perform the same transformation with vertices of physical and auxiliary fields. The coefficients depend on momentum [see Eq. (9)], and here they are put on the mass shell of the physical meson field with quantum numbers $aP0n$. Coefficients $\mathcal{O}^{ab}_{nn'}$ and masses are calculated consistently *via* diagonalization of the term (9) of the effective action and solution of Eq. (7). For η and η' mesons $\mathcal{O}^{ab}_{0n}$ mixes not only the vertices F_{n0} but also η^0 and η^8 components of the pseudoscalar nonet (15) (see Table III). In momentum representation, the vertex has the following structure:

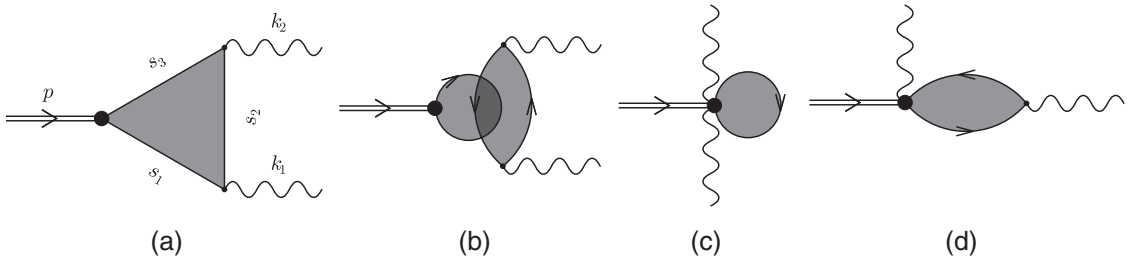

FIG. 3. Diagrams which in principle could contribute to the transition form factor. In the approximation to the quark and gluon propagators that is used in the present calculation the only nonzero contribution comes from the diagram A.

$$T^{an}_{\mu\nu}(p^2,k_1^2,k_2^2) = ie^2\delta^{(4)}(p-k_1-k_2)\varepsilon_{\mu\nu\alpha\beta}k_{1\alpha}k_{2\beta}T^{an}(p^2,k_1^2,k_2^2). \tag{16}$$

Below we shall use dimensionless notation for the masses and momenta: $p^2 \equiv p^2/\Lambda^2$, $k_1^2 \equiv k_1^2/\Lambda^2$, $k_2^2 \equiv k_2^2/\Lambda^2$, $m_f \equiv m_f/\Lambda$. Using expressions (14) and (13) for the quark propagator and quark-meson vertices, we arrive at

$$\begin{aligned} T^{an}(p^2,k_1^2,k_2^2) = {} & \frac{h_{aP0n}}{16\pi^2\Lambda}\sum_{n',f,v}\frac{1}{vn'!}\mathcal{O}^{ab}_{nn'}\mathcal{M}^{b}_{ff}q_f^2 m_f\int_0^1 ds_1\int_0^1 ds_2\int_0^1 ds_3\int_0^1 dt t^{n'}\frac{\partial^{n'}}{\partial t^{n'}} \\ & \times\left[\left(\frac{1-s_1}{1+s_1}\right)\left(\frac{1-s_2}{1+s_2}\right)\left(\frac{1-s_3}{1+s_3}\right)\right]^{m_f^2/4v}\frac{1}{(1-s_1^2)(1-s_2^2)(1-s_3^2)} \\ & \times\frac{1}{\phi^2}\left[\lambda_1\frac{F_1}{\phi^2}+\lambda_2\left(\frac{F_2}{\phi^2}+m_f^2\frac{F_3}{\phi}-p^2\frac{F_4}{\phi^3}+k_1^2\frac{F_5}{\phi^3}+k_2^2\frac{F_6}{\phi^3}\right)+\lambda_3[(p^2-k_1^2-k_2^2)^2-4k_1^2k_2^2]\frac{F_7}{\phi^4}\right] \\ & \times\exp\left\{-k_1^2\frac{\phi_{11}}{2v\phi}-k_2^2\frac{\phi_{12}}{2v\phi}-p^2\frac{\phi_1}{4v\phi}\right\}. \end{aligned} \tag{17}$$

where q_f is the electric charge of a quark with flavor f in units of electron charge. Polynomials $\phi, \phi_1, \phi_{11}, \phi_{12}$ look as

$$\begin{aligned} \phi &= s_1+s_2+s_3+s_1s_2s_3+2vt(1+s_1s_2+s_1s_3+s_2s_3), \\ \phi_1 &= (s_1-s_2+s_3-s_1s_2s_3)vt+2s_1s_3, \\ \phi_{11} &= s_2[s_1+tv(1+s_1s_3)], \\ \phi_{12} &= s_2[s_3+tv(1+s_1s_3)]. \end{aligned} \tag{18}$$

Exact expressions for momentum independent polynomials $F_i(s_1,s_2,s_3,t)$ are given in Appendix B.

Functions λ_i originate from averaging of the triangle diagram over the space-time direction of the vacuum field according to Eq. (12). Before averaging, the triangle diagram is represented by the integral over variables s_1, s_2, s_3, and t with the integrand proportional to the exponential factor

$$\begin{aligned} & \exp\{if_{\mu\nu}J_{\mu\nu}\}, \\ & J_{\mu\nu} = \frac{\phi_2(s_1,s_2,s_3,t)}{2v\phi(s_1,s_2,s_3,t)}(k_{1\mu}k_{2\nu}-k_{1\nu}k_{2\mu}), \\ & \phi_2 = s_2(s_1s_3+(s_1+s_3)tv). \end{aligned} \tag{19}$$

TABLE III. Matrix elements of the on-shell mixing matrix $\mathcal{O}_{\mathcal{Q}\mathcal{Q}'}$ for π, η, η', and η_c. For π and η_c mesons the quantities $\mathcal{O}_n^{\pi/\eta_c} \equiv \mathcal{O}_{0n}^{\pi/\eta_c}(-M^2_{\pi/\eta_c})$ characterize the weight of the vertices (13) with different radial number n in interaction of quarks with the physical ground state π and η_c mesons. For η and η' mesons mixing between octet and singlet states ($a = 0, 8$) is taken into account simultaneously with the radial number mixing.

Meson	a	$\mathcal{O}_0$	$\mathcal{O}_1$	$\mathcal{O}_2$	$\mathcal{O}_3$	$\mathcal{O}_4$	$\mathcal{O}_5$	$\mathcal{O}_6$
π	–	0.7595	−0.4510	0.3067	−0.2294	0.1826	−0.1515	0.1293
η_c	–	0.6225	−0.47789	0.3788	−0.3079	0.2554	−0.2155	0.1846
η	0	0.244	−0.1437	0.1036	−0.0812	0.0662	−0.0553	0.0471
	8	−0.6724	0.4495	−0.3189	0.2406	−0.191	0.1574	−0.1334
η'	0	+0.0139	−0.5106	0.4346	−0.2968	0.198	−0.1388	0.1049
	8	−0.6140	−0.0201	0.0985	−0.0664	0.0312	−0.0096	−0.0013

This factor is directly related to the local gauge invariance of the meson effective action with respect to the local gauge transformations of the background field which is provided by the covariant derivatives in the vertex (13) and the exponential phase factor (sometimes called the Schwinger phase) in the quark propagator (17). As a result of averaging, the final representation contains functions

$$\lambda_1(r)=\frac{\sin r}{r},\qquad \lambda_2(r)=-\frac{1}{r}\frac{\partial}{\partial r}\lambda_1(r),$$
$$\lambda_3(r)=-\frac{1}{r}\frac{\partial}{\partial r}\lambda_2(r),$$
$$r=\sqrt{2(J_{\mu\nu}J_{\mu\nu}\pm J_{\mu\nu}\tilde{J}_{\mu\nu})}=\frac{\phi_2}{v\phi}\sqrt{k_1^2k_2^2-(k_1k_2)^2}$$
$$=\frac{\phi_2}{2v\phi}\sqrt{4k_1^2k_2^2-(p^2-k_1^2-k_2^2)^2}. \tag{20}$$

For $p^2=-M^2$, that is relevant to the transition form factors, the argument r becomes imaginary $r=i\rho$,

$$\rho=\frac{\phi_2}{2v\phi}\sqrt{M^4+(k_1^2-k_2^2)^2+2M^2(k_1^2+k_2^2)}, \tag{21}$$

and one gets

$$\lambda_1=\frac{\sinh\rho}{\rho},\qquad \lambda_2=-\frac{\cosh\rho}{\rho^2}+\frac{\sinh\rho}{\rho^3},$$
$$\lambda_3=\frac{\sinh\rho}{\rho^3}-3\frac{\cosh\rho}{\rho^4}+3\frac{\sinh\rho}{\rho^5}. \tag{22}$$

Unlike the exponent with the function ϕ_1 in Eq. (17), these factors demonstrate a manifestly nonperturbative impact of the long range confining vacuum gluon fields on the behavior of form factors at short distances, as meson mass M turns out to be entangled with a highly virtual momenta of photons.

An important observation is that the behavior of the functions λ_i at large Q^2 is very different for symmetric $(k_1^2=k_2=Q^2)$ and asymmetric $(k_1^2=Q^2,\ k_2^2=0)$ kinematics since

$$\rho_{\rm sym}=\frac{\phi_2}{2v\phi}\sqrt{M^4+4M^2Q^2}\to\frac{\phi_2}{v\phi}M|Q|,$$
$$\text{for } k_1^2=k_2^2=Q^2\gg M^2,$$
$$\rho_{\rm asym}=\frac{\phi_2}{2v\phi}(M^2+Q^2)\to\frac{\phi_2}{2v\phi}Q^2,$$
$$\text{for } k_2^2=0, k_1^2=Q^2\gg M^2,$$

which results in the linear exponential increase of λ_i as a function of $|Q|$ in the integrand of the expression for the form factor in the symmetric kinematics, while quadratically growing exponents in λ_i are characteristic for the asymmetric one. Nevertheless, as it is shown in Appendix C, both regimes demonstrate $1/Q^2$ behavior for asymptotically large Q^2. However, a qualitatively different form of functions λ_i for these kinematic regimes results in a rather different degree of correspondence to factorization bound for the coefficients in front of $1/Q^2$, as is also illustrated in Fig. 4.

Below we use the notation P for a couple of indices (an). The transition form factor of meson P is defined as

$$F_{P\gamma^*\gamma}(Q^2)=T_P(-M_P^2,Q^2,0),$$

and corresponds to asymmetric kinematics with one on-shell photon. The form factor in symmetric kinematics

$$F_{P\gamma^*\gamma^*}(Q^2)=T_P(-M_P^2,Q^2,Q^2) \tag{23}$$

corresponds to two virtual photons. The decay width into a couple of real photons is expressed via decay constant $g_{P\gamma\gamma}$

$$\Gamma(P\to\gamma\gamma)=\frac{\pi}{4}\alpha^2M_P^3g_{P\gamma\gamma}^2,\quad g_{P\gamma\gamma}=T_P(-M_P^2,0,0). \tag{24}$$

Experimental and calculated by means of triangle diagram values of $g_{P\gamma\gamma}$ are given in Table IV. Results of numerical computations of transition form factors for π, η, η', and η_c mesons in comparison with experimental data are shown in Figs. 5 and 6. It should be stressed again that all calculations have been performed consistently with calculation of the masses, weak decay, and transition constants (Fig. 2 and Table II) [37].

Two-photon decay constants of π and η mesons are obtained with rather high accuracy, and overall behavior of their form factors is reproduced quite well. Moreover, high Q^2 asymptotics of the pion form factor looks more consistent with Belle data. Figure 5 manifestly demonstrates a qualitative difference between the asymmetric (solid line) and symmetric (dashed line) regimes of kinematics.

The constant value of $Q^2F_{\pi\gamma^*\gamma}(Q^2)$ is achieved at very large Q^2. It deviates from the factorization limit by more than 20% [see Eq. (2)]. At the same time, form factor $Q^2F_{\pi\gamma^*\gamma^*}(Q^2)$ approaches the asymptotic value at quite low momenta and fits the factorization limit identically, as has already been indicated in Eq. (3). Appendix C contains more detailed consideration of the asymptotic behavior of the form factor. It is explicitly demonstrated that the

TABLE IV. Two-photon decay constants of pseudoscalar mesons.

meson	$g^{\rm exp}_{P\gamma\gamma}$, GeV^{-1} [42]	$g_{P\gamma\gamma}$, GeV^{-1}
π^0	0.274	0.272
η	0.274	0.267
η'	0.344	0.44
η_c	0.067	0.055

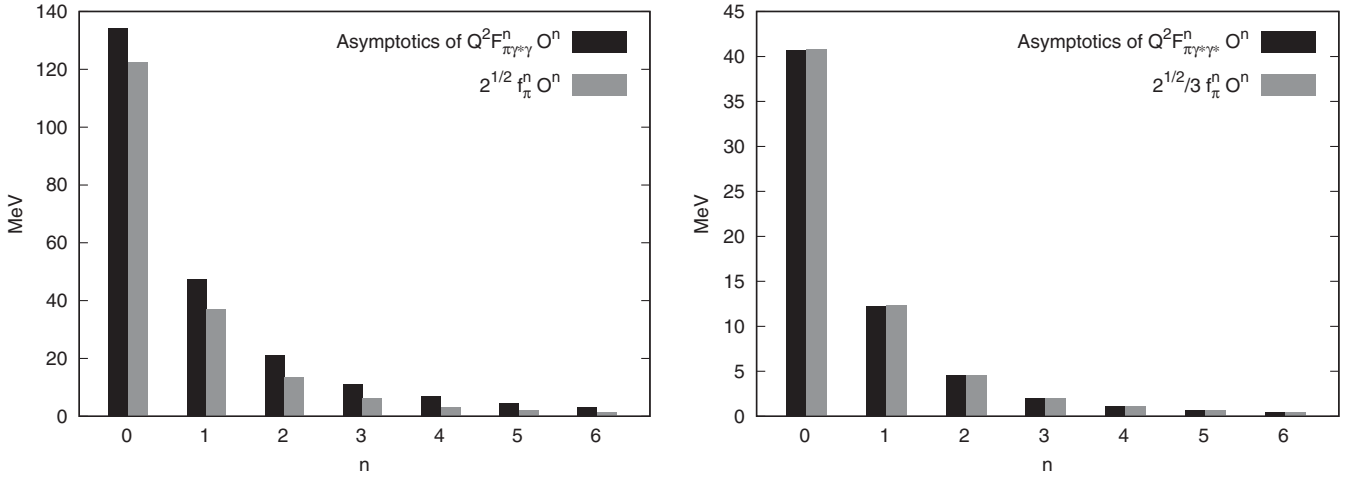

FIG. 4. Comparison of contributions to $\sqrt{2}f_\pi$ and large Q^2 asymptotics of $Q^2F_{\pi\gamma^*\gamma}$ (left), $\sqrt{2}f_\pi/3$ and asymptotics of $Q^2F_{\pi\gamma^*\gamma^*}$ (right) from meson-quark vertices (13) with various radial number n. For the sake of brevity, O^n denotes matrix elements $\mathcal{O}^{33}_{0n}$ which correspond to the ground state of π^0 that diagonalizes the quadratic part of the effective meson action. The values of these matrix elements are given in Table III.

translation noninvariant factor (19) manifestly contributes to the constant limit of $Q^2F_{\pi\gamma^*\gamma}(Q^2)$ for $Q^2 \to \infty$. This factor is completely irrelevant for the asymptotic value of $Q^2F_{\pi\gamma^*\gamma^*}(Q^2)$, which exactly reproduces the factorization bound for symmetric kinematics.

At this step we conclude that the long range confining gluon fields do not change the conventional character of the momentum dependence of the form factor but, depending on kinematic regime, may influence the coefficient in front of the $1/Q^2$ asymptotics. The coefficient coincides identically with factorization prediction in the case of symmetric kinematics in line with the analysis of papers [18–20]. Contribution of the confining Abelian (anti-)self-dual fields increases asymptotics of $Q^2F_{\pi\gamma^*\gamma}(Q^2)$ by approximately 23% in comparison with the factorization limit. This increase does not lead to contradiction with the current experimental data. If we neglect the main contribution of these long-range fields to $F_{\pi\gamma^*\gamma}$ by taking $\rho = 0$ in the integrand of (17) than the asymptotics complies with the factorization bound as well (see Appendix C). Both the two-photon decay constant and the transition form factor of the η meson turn out to be also described rather satisfactorily. These findings together with previously obtained results for masses, decay, and transition constants of various mesons and new results on strong decays (see next section) take shape of a self-consistent picture. However, consideration of η' and η_c mesons indicates that the approximation scheme used for the quark propagators

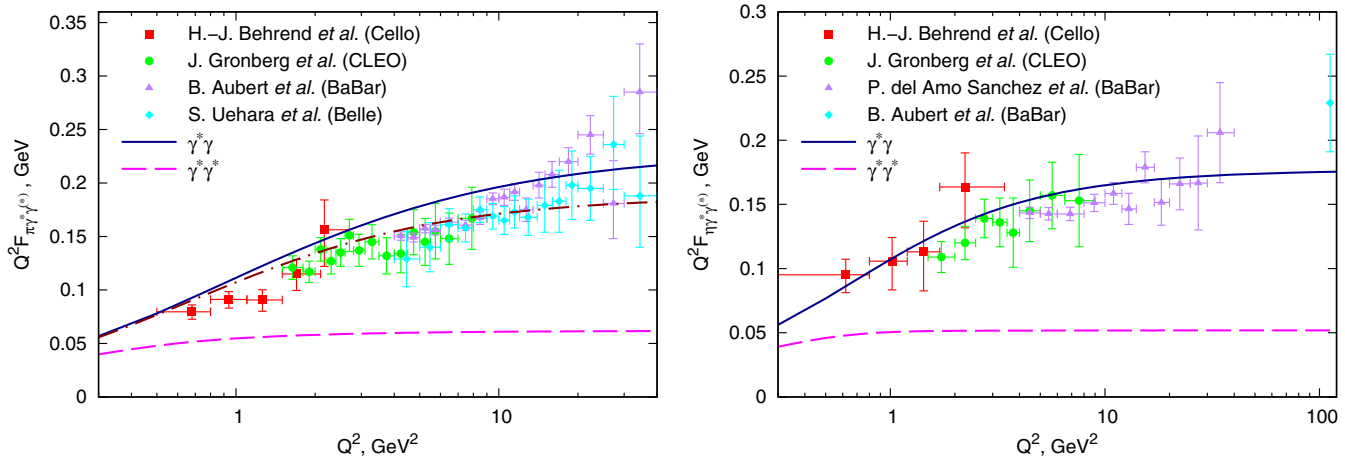

FIG. 5. Contribution of triangle diagram to the transition form factors of π and η mesons in asymmetric (solid line) and symmetric (dashed line) kinematics. The experimental data are taken from [1,3,45–47]. Dot-dashed line corresponds to $\pi \to \gamma^*\gamma$ transition calculated without taking into account the main contribution of the background field encoded in λ-functions, which agrees very well with Eq. (1) (for details see Appendix C).

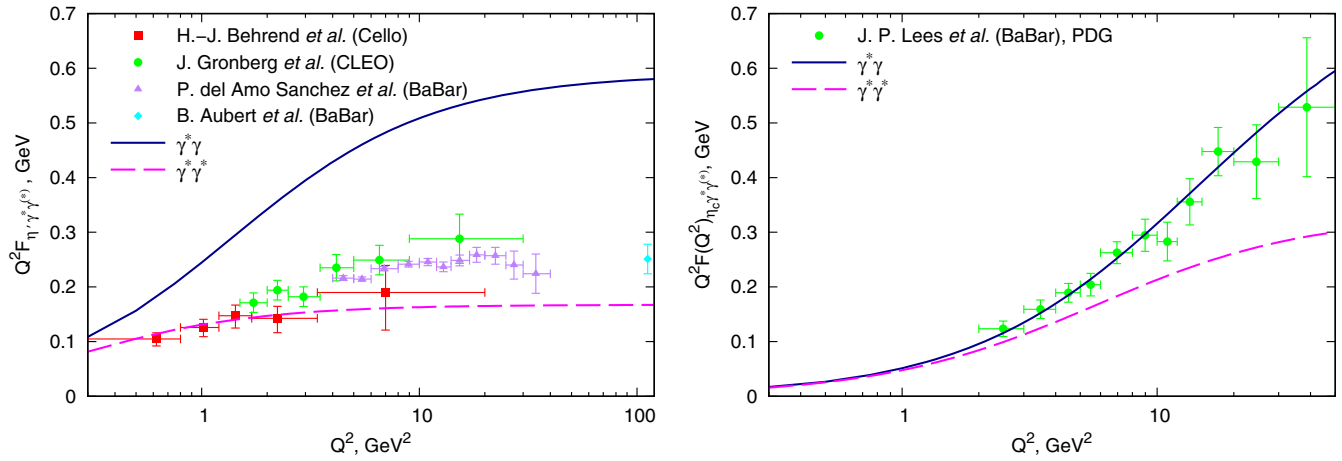

FIG. 6. Contribution of triangle diagram to the transition form factor for η' (left) and η_c (right) mesons in asymmetric kinematics (solid line) and symmetric kinematics (dashed line). Experimental data are taken from papers [1,45–47].

in the domain wall network background has to be refined by explicitly taking into account the inhomogeneity of the background field at domain boundaries. Without implementation of this technically complicated enhancement, the picture appears to be incomplete. We shall discuss this difficult issue in the last section of the paper.

IV. STRONG DECAYS OF VECTOR MESONS

Analysis of the previous section emphasized the important role of long range confining gluon fields and related local gauge invariance of the meson effective action in formation of the transition form factors. Strong decays of vector mesons allow one to verify the validity of such an emphasis.

The amplitude of vector meson decay into a couple of pseudoscalar mesons includes two form factors,

$$A_\mu = 2q_\mu A_1(p^2,q^2,pq) + p_\mu A_2(p^2,q^2,pq),$$

where p_μ is momentum of the decaying meson, and $q_\mu = k_{1\mu} - k_{2\mu}$ is the relative momentum of pseudoscalar mesons. The corresponding decay constant is defined as the on-shell form factor

$$g_{VPP} = A_1(p^2,q^2,pq), \qquad p^2 = -M_1^2,$$
$$k_1^2 = -M_2^2, \qquad k_1^2 = -M_3^2.$$

The diagram for the amplitude A_μ shown in Fig. 8 for ground state mesons corresponds to the expressions

$$A^\mu_{aV,bP,cP}(p,k_1,k_2) = h_{aV00}h_{bP00}h_{cP00}\sum_{n_1n_2n_3}\mathcal{O}^a_{0n_1}(p)\mathcal{O}^b_{0n_2}(k_1)\mathcal{O}^c_{0n_3}(k_2)\tilde{\Gamma}^\mu_{aVn_1,bPn_2,cPn_3}(p,k_1,k_2),$$

$$\Gamma^\mu_{aVn_1,bPn_2,cPn_3}(x,y,z) = \int d\sigma_B \mathrm{Tr}\gamma^\mu \mathcal{M}^a F_{n_1}(x)S(x,y)i\gamma_5\mathcal{M}^b F_{n_2}(y)S(y,z)i\gamma_5\mathcal{M}^c F_{n_3}(z)S(z,x),$$

where we have written flavor multiplet indices (a,b,c) explicitly. In this case matrices $\mathcal{O}$ are diagonal with respect to multiplet indices, which is denoted by a single index. The final result for the decay constant has the following general structure:

$$g_{VP_1P_2} = h_V h_{P_1} h_{P_2}\int_0^1\int_0^1\int_0^1\int_0^1\int_0^1\int_0^1 ds_1ds_2ds_3dt_1dt_2dt_3\left(\frac{1-s_1}{1+s_1}\right)^{\frac{m_1^2}{4v}}\left(\frac{1-s_2}{1+s_2}\right)^{\frac{m_2^2}{4v}}\left(\frac{1-s_3}{1+s_3}\right)^{\frac{m_3^2}{4v}}$$
$$\times\exp\left(\sum_{i=1}^3\phi_i M_i^2\right)\left[\lambda_1+\lambda_1\sum_{i=1}^3 F_{1i}M_i^2+\lambda_2\left(\sum_{i=1}^3 F_{2i}M_i^2+\sum_{\substack{i,j=1,2,3\\ i\le j}}F_{3ij}M_i^2M_j^2\right)+\lambda_3\sum_{\substack{i,j,k=1,2,3\\ i\le j\le k}}F_{4ijk}M_i^2M_j^2M_k^2\right],$$

where M_1 is the mass of the vector meson, M_2 and M_3 are masses of pseudoscalar mesons, and ϕ and F are rational functions of integration variables s_i and t_i independent of the meson masses. Quark masses m_f correspond to the flavor content of the mesons.

TABLE V. The strong decay $V \to PP$ constants for various decays. Here g_{VPP} is the result of the full calculation with locally gauge invariant meson-meson amplitudes, and g^*_{VPP} is a simplified, only globally gauge invariant calculation.

Decay	$g^{\rm exp}_{VPP}$ [42]	g_{VPP}	g^*_{VPP}
$\rho^0 \to \pi^+\pi^-$	5.95	7.61	1.14
$\omega \to \pi^+\pi^-$	0.17	0	0
$K^{*\pm} \to K^\pm\pi^0$	3.23	3.56	0.65
$K^{*\pm} \to K^0\pi^\pm$	4.57	5.03	0.91
$\varphi \to K^+K^-$	4.47	5.69	1.11
$D^{*\pm} \to D^0\pi^\pm$	8.41	7.94	16.31
$D^{*\pm} \to D^\pm\pi^0$	5.66	5.62	11.53

Functions $\lambda_i(\zeta)$ are given by the same Eq. (20) as in the case of two-photon decay of pseudoscalar mesons but now with the argument

$$\zeta = \psi\sqrt{(M_1^2 - M_2^2 - M_3^2)^2 - 4M_2^2M_3^2},$$

where ψ is a function of the integration variables, which obviously differs from the corresponding function in Eq. (21).

The origin and physical content of the λ-functions discussed above in the context of the transition form factors is completely applicable to the strong $V \to PP$ decays as well. An important observation is that these functions turn out to be of crucial importance for an adequate description of the experimental results for $V \to PP$ decay constants. The results are shown in Table V. The value of $g_{\omega\pi\pi}$ is exactly zero in our calculation because of ideal mixing of ω and ϕ mesons and employed approximation of $SU(2)$ isospin symmetry ($m_u = m_d$). If one neglects translation noninvariant phases in the quark propagator and drops the background field dependence in the quark-meson vertices, that means turning to just global gauge invariance of meson-meson interaction vertices, then the argument of λ_i has to vanish $\xi \to 0$, and the results of the calculation change dramatically as is seen from comparison of the third and fourth columns in Table V. The calculated decay constants become strongly underestimated for light mesons and overestimated for heavy-light mesons. This is quite a known issue—it is difficult to get a consistent description of both meson masses and strong decay constants. Usually $g_{\rho\pi\pi}$ turns out to be strongly underestimated [40,41].

The main observation of this section is that the local gauge invariance of the meson effective action is highly important for a simultaneous description of meson masses and the strong decay constants g_{VPP}. This conclusion supports the analysis of the impact of the confining long range gluon fields on $P \to \gamma\gamma$ transition form factors.

V. DISCUSSION AND OUTLOOK

Two-photon decay constants for η_c and, particularly, η' mesons turn out to deviate from experimental values by 18% and 24%, respectively, which demonstrates much less accuracy of description than in the case of π and η mesons. At a glance the η_c form factor in Fig. 6, calculated by means of Eq. (17), fits experimental data very well. However, the normalized at zero momentum form factor shown in Fig. 7 exposes its functional form more clearly, and, though an agreement is still quite reasonable, there is a visible excess of the calculated form factor with respect to the experimental points. Bearing in mind 18% underestimation of $g_{\eta_c\gamma\gamma}$ we conclude that a good description seen in Fig. 6 is a result of mutual compensation of two inaccuracies. Equation (17) leads to a strong overestimation of the normalized form factor of the η' meson as the left-hand side plot in Fig. 7 demonstrates. Simultaneously the decay constant $g_{\eta'\gamma\gamma}$ exceeds the experimental value. The left-hand side plot in Fig. 6 demonstrates the heavy overall disagreement of $Q^2F_{\eta'\gamma^*\gamma}(Q^2)$ with experimental data.

Bearing in mind systematically good accuracy of the present approach in the description of diverse properties of various mesons, one gets an impression that the odd situation

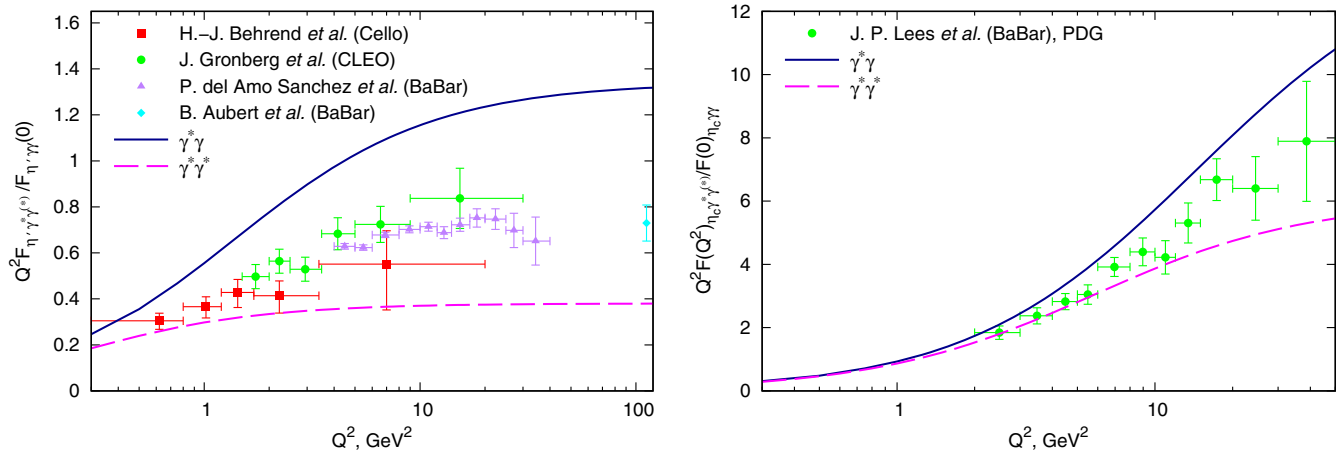

FIG. 7. Contribution of triangle diagram to the transition form factors for η' and η_c mesons normalized at $Q^2 = 0$ and multiplied by Q^2. The experimental data are taken from [1,45–47] and [48] respectively. Such normalization allows one to present and compare the overall shapes of calculated and experimentally measured form factors in a clear way. Mismatch of decay constants is compensated in this representation.

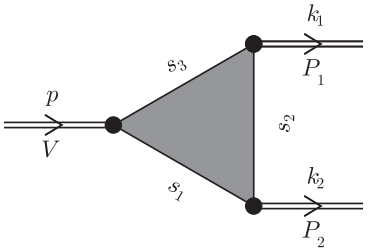

FIG. 8. Diagram for the three-point meson interaction vertex. Gray background denotes averaging over background vacuum field.

with η' has to be attributed to some effects, that are particularly important for η' meson. If so then it can be plausible that the triangle diagram A in Fig. 3 does not represent all potentially important contributions to the transition form factor, which are specifically large in the case of the η' meson.

It is known that within the instanton liquid model the analogue of diagram B gives an important contribution to the transition form factor $F_{P\gamma^*\gamma}$; under certain conditions it can become as large as the contribution of the triangle diagram. A detailed analysis of the direct instanton effects in the pion transition form factor was performed in paper [26]. It was shown that if flavor $SU(2)$ symmetry is broken due to different current masses of up and down quarks then direct instanton effects are not small and may lead to a considerable increase of the pion form factor at large Q^2. The addition to the form factor is equal to the difference of two terms related to the up and down quarks, which together with other factors define its overall sign. Obviously for unbroken flavor $SU(2)$ symmetry, this effect vanishes.

This approach can be extended to all pseudoscalar neutral mesons. Contribution of the diagram B to the form factors of the η^8 and η^0 states is expected to be nonzero for broken $SU(3)$ flavor symmetry. However there is an important difference between octet and singlet states. Contribution to the η^8 form factor is given by the difference of terms related to the light quarks and the s-quark, while addition to the η^0 form factor is given by a sum of terms and does not vanish even for the case of unbroken $SU(3)$. This means that the strongest effect can be expected for the case of η^0 with a sign being opposite to the sign of octet states. In other words, contribution of diagram B may increase the form factors of octet states and decrease the η^0 and η_c form factors. The same as for the η^0 state argumentation is applicable to the η_c meson form factor but in a much more smeared form due to the large c-quark mass.

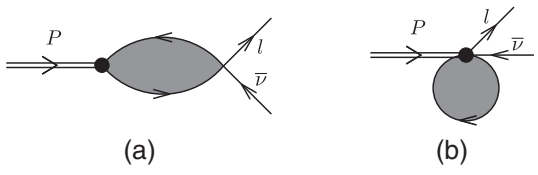

FIG. 9. Diagrams for the weak decay constant of charged pseudoscalar mesons.

In the present approach, the η^0 and η^8 ground and radially excited states are mixed with each other to form the physical η, η' mesons and their physical radial excitations. Mixing with η_c is negligible. Physical meson fields diagonalize the quadratic part of the effective action (6). Table III demonstrates the on-shell coefficients of the mixing. It should be noted that on-shell singlet-octet mixing cannot be described by one or two mixing angles since the presence of radially excited modes requires a much more complicated parametrization expressed in terms of the transformation $\mathcal{O}$ (for details see [37]). Here it is important to note that both diagrams shown in Fig. 1 contribute to the mixing. The right-hand side diagram includes a two-point correlator of the background gluon fields that is particularly crucial for the description of the η and η' masses. The diagram B in Fig. 3 is akin to the right-hand side diagram in Fig. 1. The simplified scheme for taking into account the finite size of domains in terms of the background field correlators has been sufficient for estimation of η and η' masses, but it appears to be unable to catch the contribution to the form factor potentially arising from the diagram B. Being locally (color) gauge invariant, the quark polarization two-point subdiagram is translation invariant despite the presence of translation noninvariant phases in the quark propagators. As a result of this, the tensor structure (16), generated initially by the presence of the (anti-)self-dual background gluon field, turns out to be eliminated by the energy-momentum conservation in the polarization loop separately from the whole diagram.

Thus we conclude that the effect of direct correlations of the vacuum fields encoded in diagam B in Fig. 3 is missed in our present calculation due to the oversimplified approximation used for the quark propagators in the presence of the domain structured background gluon field. Namely, the propagator in the bulk of the domain with finite size is approximated by the propagator in the infinite space-time. This appears to be an excessive simplification: the latter propagator is translation invariant up to an appropriate gauge transformation, while the lack of translation invariance in the former one relates also to the finite size and random space-time position of a given domain. In principle this mismatch can be improved by the use of the quark propagator represented in terms of quark eigenmodes inside the finite domain filled by the Abelian (anti-)self-dual homogeneous gluon field analytically obtained in paper [44]. At least an estimation based on the few lowest eigenmodes (analogous to the analysis of [26]) seems to be a technically realistic task to be tackled in due course.

ACKNOWLEDGMENTS

We acknowledge fruitful discussions with A. Dorokhov, S. Mikhailov, N. Kochelev, O. Teryaev, and T. N. Pham for valuable comments. Research presented in this paper was funded by the Joint Institute for Nuclear Research.

APPENDIX A: HADRONIZATION WITHIN THE DOMAIN MODEL OF QCD VACUUM

Nonperturbative gluon fields are represented in the model by the ensemble of domain-structured fields with the field strength tensor [34–36]

$$F^a_{\mu\nu}(x) = \sum_{k=1}^{N} n^{(k)a} B^{(k)}_{\mu\nu} \theta(1-(x-z_k)^2/R^2),$$

$$B^{(k)}_{\mu\nu} B^{(k)}_{\mu\rho} = B^2 \delta_{\nu\rho}, \qquad B = \frac{2}{\sqrt{3}}\Lambda^2,$$

$$\tilde{B}^{(k)}_{\mu\nu} = \pm B^{(k)}_{\mu\nu}, \qquad \hat{n}^{(k)} = t^3 \cos\xi_k + t^8 \sin\xi_k,$$

$$\xi_k \in \left\{ \frac{\pi}{6}(2l+1), l = 0, \ldots, 5 \right\},$$

where scale Λ and mean domain radius R are parameters of the model related to the scalar gluon condensate and topological susceptibility, respectively, $B_{\mu\nu}$ is a constant (anti-)self-dual tensor for the field strength in kth domain, and $\theta(1-(x-z_k)^2/R^2)$ is a characteristic function of the kth domain.

The measure of integration over the ensemble of background fields is defined as

$$\int_{\mathcal{B}} d\sigma_B \ldots = \prod_i \frac{1}{24\pi^2} \int_V \frac{d^4 z_i}{V} \int_0^{2\pi} d\varphi_i \int_0^{\pi} d\theta_i \sin\theta_i \times \int_0^{2\pi} d\xi_i \sum_{l=0,1,2}^{3,4,5} \delta\left(\xi_i - \frac{(2l+1)\pi}{6}\right) \times \int_0^{\pi} d\omega_i \sum_{k=0,1} \delta(\omega_i - \pi k) \ldots,$$

where angles φ_i, θ_i characterize direction of the chromomagnetic field, ω_i is the angle between the chromomagnetic and chromoelectric fields, and ξ_i describes the color "orientation" of the background filed in the ith domain, centered at the space-time point z_i.

Recalling the definition of the n-point Green's functions for QCD in the presence of the background field B,

$$G^{a_1\ldots a_n}_{\mu_1\ldots\mu_n}(x_1,\ldots,x_n|B) = \frac{1}{g^n} \frac{\delta^n \ln W[j]}{\delta j^{a_1}_{\mu_1}(x_1)\ldots\delta j^{a_n}_{\mu_n}(x_n)}\bigg|_{j=0},$$

where $W[j]$ is the generating functional, one may integrate out ghost and gluon field fluctuations and arrive at the representation for QCD functional integral in the background gauge

$$\mathcal{Z} = N \int d\sigma_B \int_\Psi \mathcal{D}\psi\mathcal{D}\bar{\psi} \exp\left\{ \int dx \bar{\psi}(i\partial + gB - m)\psi \right\} W[J],$$

$$W[J] = \exp\left\{ \sum_n \frac{g^n}{n!} \int d^4x_1 \ldots \int d^4x_n j^{a_1}_{\mu_1}(x_1)\ldots j^{a_n}_{\mu_n}(x_n) G^{a_1\ldots a_n}_{\mu_1\ldots\mu_n}(x_1,\ldots,x_n|B) \right\},$$

where $j^a_\mu(x) = \bar{\psi}(x)\gamma_\mu t^a \psi(x)$ is the quark current. By construction the gauge coupling constant g here appears to be renormalized within some appropriate renormalization scheme, and the n-point correlators are exact renormalized n-point gluon Green functions of pure gauge theory in the presence of the background field B. Needless to say, the exact form of the Green functions is not known, and certain reliable approximations have to be introduced. We truncate the exponent in $W[j]$ up to the four-fermion interaction term and approximate the two-point correlation function by the gluon propagator in the presence of homogeneous Abelian (anti-)self-dual field neglecting radiative perturbative corrections. The randomness of the domain ensemble is taken into account implicitly by means of averaging the quark loops over all possible configurations of the homogeneous background field at the final stage of derivation of the effective meson action [34,35]. The approximated functional integral reads

$$\mathcal{Z} = \int_{\mathcal{B}} dB \int_\Psi \mathcal{D}\psi\mathcal{D}\bar{\psi} \exp\left\{ \int d^4x \bar{\psi}(i\partial + gB - m)\psi + \mathcal{L} \right\},$$

$$\mathcal{L} = \frac{g^2}{2} \int d^4x \int d^4y G^{ab}_{\mu\nu}(x,y|B) j^a_\mu(x) j^b_\nu(y), \tag{A1}$$

where m is a diagonal quark mass matrix. By means of the Fiertz transformation of color, Dirac and flavor matrices, the four-quark interaction can be rewritten as

$$\mathcal{L} = \frac{g^2}{2} \sum_{c,J} C_J \int d^4x \int d^4y D(x-y) J^{Jc}(x,y|B) J^{Jc}(y,x|B),$$

where numerical coefficients C_J are different for different spin-parity $J = S, P, V, A$. Here bilocal color neutral quark currents

$$J^{Jc}(x,y|B) = \bar{\psi}^{if}_\alpha(x) \lambda^c_{ff'} \Gamma^{\alpha\alpha'}_J \left[\left\{ \frac{i}{2} x_\mu \hat{B}_{\mu\nu} y_\nu \right\} \right]^{ii'} \psi^{i'f'}_{\alpha'}(y)$$

are singlets with respect to the local background gauge transformations, $\hat{B}_{\mu\nu}$ denotes background field strength in the fundamental representation, and i, f, and α are color, flavor, and space-time indices respectively. In the center of quark mass coordinate system, bilocal currents take the form

$$J^{Jc}(x,y|B) \to J^{Jc}(x,z|B) = \bar{\psi}^{if}_{\alpha}(x) t^{c}_{ff'} \Gamma^{\alpha\alpha'}_{J} \times [\exp\{iz_\mu \overleftrightarrow{\mathcal{D}}_\mu(x)\}]^{ii'}_{ff'} \psi^{i'f'}_{\alpha'}(x),$$

$$\overleftrightarrow{\mathcal{D}}^{ff'}_{\mu}(x) = \xi_f \overleftarrow{\mathcal{D}}_\mu(x) - \xi_{f'} \overrightarrow{\mathcal{D}}_\mu(x),$$

$$\xi_f = \frac{m_f}{m_f + m_{f'}}, \xi_{f'} = \frac{m_f}{m_f + m_{f'}},$$

and their interaction is described by the action

$$\mathcal{L} = \frac{g^2}{2} \sum_{c,J} C_J \int d^4x \int d^4z D(z) J^{\dagger}_{Jc}(x,z|B) J_{Jc}(x,z|B), \tag{A2}$$

$$D(z) = \frac{1}{4\pi^2 z^2} \exp\left\{-\frac{1}{4}\Lambda^2 z^2\right\}, \tag{A3}$$

where x_μ is the center of mass coordinates, and z_μ represents the relative coordinates of quark and antiquark and $\Lambda^2 = \sqrt{3}B/2$. Function $D(z)$ originates from the gluon propagator in the presence of the homogeneous Abelian (anti-)self-dual gluon field. It differs from the free massless scalar propagator by the Gaussian exponent, which completely changes the IR properties of the propagator. In momentum representation it takes the form

$$G(p^2) = \frac{1}{p^2}(1 - e^{-p^2/\Lambda^2}).$$

There are two equivalent ways to derive an effective meson action based on the functional integral (A1) with the interaction term $\mathcal{L}$ taken in the form (A2). The first one is a bosonization of the functional integral in terms of bilocal mesonlike fields. Another, more transparent in our opinion, way is to decompose the bilocal currents over a complete set of functions $f^{nl}_{\mu_1\ldots\mu_l}(z)$ characterized by the radial quantum number n and orbital momentum l and orthogonal with the weight determined by the gluon propagator (A3) in Eq. (A2),

$$J^{aJ}(x,z) = \sum_{nl} (z^2)^{l/2} f^{nl}_{\mu_1\ldots\mu_l}(z) J^{aJln}_{\mu_1\ldots\mu_l}(x).$$

The choice of functions $f^{nl}(z)$ is unambiguously determined by the gluon propagator

$$f^{nl}_{\mu_1\ldots\mu_l} = L_{nl}(z^2) T^{(l)}_{\mu_1\ldots\mu_l}(n_z), \qquad n_z = z/\sqrt{z^2}, \tag{A4}$$

where $T^{(l)}_{\mu_1\ldots\mu_l}$ are irreducible tensors of the four-dimensional rotational group, and generalized Laguerre polynomials L_{nl} obey the relation

$$\int_0^\infty du \rho_l(u) L_{nl}(u) L_{n'l}(u) = \delta_{nn'}, \qquad \rho_l(u) = u^l e^{-u}. \tag{A5}$$

The weight $\rho_l(u)$ originates from the gluon propagator (A3). Nonlocal quark currents $J^{aJln}_{\mu_1\ldots\mu_l}$ with a complete set of meson quantum numbers depend only on the center of mass coordinate x [33,35],

$$J^{aJln}_{\mu_1\ldots\mu_l}(x) = \bar{q}(x) V^{aJln}_{\mu_1\ldots\mu_l}\left(\frac{\overleftrightarrow{D}(x)}{\Lambda}\right) q(x).$$

An explicit form of the vertex operator $V^{aJln}_{\mu_1\ldots\mu_l}$ is given in (13). The four-fermion interaction takes the form

$$\mathcal{L} = \frac{g^2}{2} \sum_{a,J,l,n} C_J \int d^4x J^{\dagger}_{aJln}(x) J_{aJln}(x).$$

Details of decomposition of bilocal quark currents and the bosonization procedure can be found in [33,35]. By means of bosonization, the truncated QCD functional integral can be rewritten as the integral over composite colorless mesonlike fields Φ given in (5).

APPENDIX B: TRANSITION FORM FACTOR

Polynomial functions $F_i(s_1,s_2,s_3,t)$ in Eq. (17) have the following form:

$$\begin{aligned}
F_1 = {} & -2(2s_1^4(2(s_2-1)(s_2+1)t^2v^2(s_2^2(s_3^2-2)+s_2s_3(s_3^2-1)+s_3^2(2s_3^2-1)) \\
& + tv(s_2^4s_3(s_3^2-4) - 2s_2^3(s_3^4-s_3^2+1) + s_2^2s_3(s_3^2+3) + 2s_2s_3^2 - 2s_3^3 + s_3) \\
& - -s_2s_3(s_2-s_3)(s_2+s_3)(s_2s_3+1)) + s_1^3((s_2-1)(s_2+1)tv(s_2^2(5s_3^4+3s_3^2-4) \\
& + s_2(5s_3^2-9)s_3 + 4s_3^4 - 4s_3^2 - 2) + 2(s_2-1)(s_2+1)t^2v^2(5s_2^2(s_3^2-1)s_3 + s_2(s_3^4+s_3^2-2) + 6s_3^3 - 4s_3) \\
& + 2(s_2(-s_2^3s_3 + 2s_2(s_2^2-1)s_3^3 - (s_2^2+1)s_3^2 + s_3^4 + 1) + s_3)) + s_1^2(2s_2^4s_3^2 - 2s_2^2(s_3^4+3s_3^2-2) \\
& + 2(s_2-1)(s_2+1)t^2v^2(s_2^2(3s_3^4-s_3^2+2) + s_2(s_3-s_3^3) - 2s_3^4 + 2s_3^2 - 2) + tv(4(s_2^3+s_2) \\
& + s_2(3s_2^2+5)s_3^4 - s_2(7s_2^2+9)s_3^2 + (7s_2^4 - 11s_2^2 + 4)s_3^3 + (s_2^4 - 3s_2^2 + 2)s_3) - 4s_2s_3(s_3^2-1) + 4s_3^2 - 2) \\
& + 2s_1(s_2^4(-s_3^3) - s_2^3s_3^4 + s_2^3s_3^2 + s_2^3 - 2(s_2-1)(s_2+1)t^2v^2((2s_2^2+3)s_3^3 - 2(s_2^2+1)s_3 + s_2s_3^4 - s_2) \\
& - (s_2-1)(s_2+1)tv(s_2^2(3s_3^4-1) + s_2(3s_3^2-5)s_3 + s_3^4 + 2s_3^2 - 4) + 2s_2^2s_3 + s_2s_3^2 - 2s_2 + s_3^3 - 2s_3) \\
& + 2tv(s_2^4(s_3 - 2s_3^3) + 2s_2^3(-s_3^4 + s_3^2 + 1) + 3s_2^2s_3 + 2s_2(s_3^2-2) + 2s_3(s_3^2-2)) \\
& - 4(s_2-1)(s_2+1)t^2v^2(s_3(s_2(s_2(2s_3^2-1)s_3 + s_3^2 - 1) + 2s_3) - 2) + 2(s_2+s_3)^2(s_2s_3-1))
\end{aligned}$$

$$
\begin{aligned}
F_2 = {} & -2(2((2(s_3^2-3)s_3^2-(7s_3^2+4)tvs_3+2(2-5s_3^2)t^2v^2)s_2^4+(s_3(4s_3^2+6(s_3^2-1)tvs_3 \\
& +6(s_3^2-1)t^2v^2-5)-2tv)s_2^3+(4s_3^4+2s_3^2+(13s_3^2+7)tvs_3+4(s_3^4+2)t^2v^2+1)s_2^2 \\
& +(s_3^3-14(s_3^2-1)t^2v^2s_3+2(-2s_3^4+s_3^2+2)tv)s_2-3s_3(s_3+tv)(2s_3tv+1))s_1^4 \\
& +(2s_3(6s_3^2-5)s_2^4+2(4s_3^4-5s_3^2+2)s_2^3+(8s_3^3-4s_3)s_2^2+2(s_3^4-s_3^2-1)s_2-12s_3^3 \\
& +2(-17s_3(s_3^2-1)s_2^4+3(s_3^4+s_3^2-2)s_2^3+s_3(11-5s_3^2)s_2^2+(-11s_3^4-3s_3^2+14)s_2 \\
& +6s_3(s_3^2-2))t^2v^2+6s_3-(s_2-1)(s_2+1)(-12s_3^4+s_2(27-31s_3^2)s_3+s_2^2(5s_3^4-13s_3^2+4)-6)tv)s_1^3 \\
& +((-6s_3^4+10s_3^2+(25s_3^2-1)tvs_3-2(7s_3^4-29s_3^2+10)t^2v^2+2)s_2^4 \\
& -(s_3^2-1)(4tv+s_3(3tv(5s_3+2tv)+4))s_2^3-(s_3(17tv+s_3(2s_3^2+25tvs_3+6(s_3^2+5)t^2v^2+6))+4)s_2^2 \\
& +(s_3^2-1)(12tv+s_3(tv(7s_3+6tv)-8))s_2-12(s_3^4-3s_3^2+1)t^2v^2-6s_3^2(s_3^2-2)+18s_3tv)s_1^2 \\
& +2(-5s_3^3s_2^4+4s_3s_2^4-5s_3^4s_2^3+5s_3^2s_2^3-s_3^2-2s_3^3s_2^2+s_3^2s_2+3s_3^3+2(10s_3(s_3^2-1)s_2^4-3(s_3^4-1)s_2^3 \\
& +s_3(s_3^2-4)s_2^2+7(s_3^4-1)s_2-3s_3^3+6s_3)t^2v^2-(s_2-1)(s_2+1)((s_2^2-3)s_3^4+9s_2s_3^3+2(s_2^2+6)s_3^2 \\
& -7s_2s_3-s_2^2)tv)s_1+2s_2(s_3(s_2s_3-1)(s_2+s_3)^2+2(2s_2(s_2^2+2)s_3^4+(7-3s_2^2)s_3^3-s_2(5s_2^2+3)s_3^2 \\
& +(3s_2^2-7)s_3+2s_2)t^2v^2+(4s_3^4-6s_3^2+s_2(2s_3^2-1)s_3+s_2^3(s_3-2s_3^3)+2s_2^2(-s_3^4+s_3^2+1))tv))
\end{aligned}
$$

$$
F_3 = \frac{4}{v}(s_1(s_2-s_3)+s_2s_3-1)(s_1s_2s_3+s_1+s_2+s_3)(tv(s_1+s_3)+s_1s_3)s_2
$$

$$
\begin{aligned}
F_4 = {} & -\frac{1}{v}2s_2(s_1(s_2-s_3)+s_2s_3-1)(tv(s_1+s_3)+s_1s_3)(s_1^3s_2^3s_3^3+s_1^3s_2^2s_3^2-2s_1^3s_2s_3^3+s_1^3s_2s_3-2s_1^3s_3^2+s_1^3 \\
& +s_1^2s_2^3s_3^2+s_1^2s_2^2s_3^3+2tv(s_1s_2s_3+s_1+s_2+s_3)(s_1^2(s_2(s_3(s_2-2s_3)+2)-s_3) \\
& +s_1(s_2^2-1)(s_3^2-1)-s_2(s_3(s_2-2s_3)+2)+s_3)+2(s_1^2-1)(s_3^2-1)t^2v^2(s_2s_3(s_1(s_2^2-3)-3s_2) \\
& -3s_1s_2^2+s_1+s_2^3-3s_2+s_3)-2s_1^2s_2s_3^2+s_1^2s_2-2s_1^2s_3^3+s_1^2s_3-s_1s_2^3s_3-s_1s_2^2 \\
& +s_1s_2s_3^3+s_1s_3^2-s_2^3-s_2^2s_3+s_2s_3^2+s_3^3)
\end{aligned}
$$

$$
\begin{aligned}
F_5 = {} & -\frac{1}{v}2s_2(s_1(s_2-s_3)+s_2s_3-1)(tv(s_1+s_3)+s_1s_3)(-s_1^3s_2^3s_3^3+2s_1^3s_2^3s_3-s_1^3s_2^2s_3^2+2s_1^3s_2^2-s_1^3s_2s_3 \\
& -s_1^3-s_1^2s_2^3s_3^2+2s_1^2s_2^3-s_1^2s_2^2s_3^3+4(s_1^2-1)s_2(s_3^2-1)t^2v^2(s_1(s_2^2-2)s_3-s_1s_2+s_2^2-s_2s_3-2) \\
& +2tv(s_1s_2s_3+s_1+s_2+s_3)(s_1^2(s_2(s_3(s_2-2s_3)+2)-s_3)-s_1(s_2^2-1)(s_3^2-1) \\
& -s_2(s_3(s_2-2s_3)+2)+s_3)+2s_1^2s_2^2s_3-s_1^2s_2-s_1^2s_3-s_1s_2^3s_3-s_1s_2^2+s_1s_2s_3^3+s_1s_3^2-s_2^3-s_2^2s_3+s_2s_3^2+s_3^3)
\end{aligned}
$$

$$
F_6(s_1,s_2,s_3,t) = F_5(s_3,s_2,s_1,t)
$$

$$
\begin{aligned}
F_7 = {} & -\frac{1}{2v^2}s_2^2(tv(s_1+s_3)+s_1s_3)^2(2s_1^4(s_2^4s_3(s_3(tv(3s_3+2tv)+2)+2tv)+s_2^3s_3(1-2tv(3(s_3^2-1)tv \\
& +s_3(s_3^2-2)))+s_2^2(-2s_3^4-(5s_3^2+3)s_3tv-4(s_3^4-s_3^2+1)t^2v^2-1)+s_2(-s_3^3+6(s_3^2-1)s_3t^2v^2-2tv) \\
& +s_3(s_3+tv)(2s_3tv+1))+s_1^3(2(s_2-1)(s_2+1)t^2v^2(3s_2^2s_3(s_3^2-1)-s_2(5s_3^4+s_3^2-6)+2s_3(s_3^2-2)) \\
& +(s_2-1)(s_2+1)tv(s_2^2(3s_3^4+s_3^2)+s_2(9-5s_3^2)s_3-4s_3^4-2)+2(s_2^4s_3+s_2^3(3s_3^2-2)-2s_2^2s_3^3 \\
& -s_2(s_3^4+s_3^2-1)+2s_3^3-s_3))+s_1^2(s_2^4(-(3s_3^2+5)s_3tv+2(s_3^2-1)s_3^2+2(s_3^4-7s_3^2+2)t^2v^2-2) \\
& +s_2^3s_3(s_3^2-1)(tv(9s_3+2tv)+4)+s_2^2((3s_3^2+11)s_3tv+2(s_3^2-1)s_3^2+2(5s_3^4-3s_3^2+4)t^2v^2+4) \\
& -s_2(s_3^2-1)tv(s_3^2+2s_3tv+8)+2s_3^2(s_3^2-2)+4(s_3^4-3s_3^2+1)t^2v^2-6s_3tv) \\
& +2s_1(s_2^4s_3^3-2s_2^4s_3+s_2^3s_3^4-3s_2^3s_3^2+s_2^3+(s_2-1)(s_2+1)tv(s_2^2(s_3^4-2s_3^2-1)+s_2(3s_3^2-5)s_3-s_3^4+4s_3^2) \\
& -2(s_2-1)(s_2+1)t^2v^2(2s_2^2(s_3^2-1)s_3-3s_2(s_3^4-1)+s_3^3-2s_3)+2s_2^2s_3+s_2s_3^2-s_3^3) \\
& -2s_2tv(s_2(s_2^2-1)s_3+2s_2^2+2s_3^4-4s_3^2)+4s_2t^2v^2(3(s_2^2-1)s_3^3+s_2(s_2^2+3)s_3^2-3(s_2^2-1)s_3 \\
& -2s_2s_3^4-2s_2)-2s_2s_3(s_2+s_3)^2(s_2s_3-1)).
\end{aligned}
$$

APPENDIX C: ASYMPTOTIC BEHAVIOR OF THE FORM FACTOR

In essence, calculation of the asymptotic behavior of the form factor (17) at $p^2=-M^2$ is reduced to consideration of the integral

$$I^{fn}(M^2,k_1^2,k_2^2)=\int_0^1 ds_1\int_0^1 ds_2\int_0^1 ds_3\int_0^1 dt t^n\frac{\partial^n}{\partial t^n}\exp\left\{-\frac{k_1^2\phi_{11}+k_2^2\phi_{12}}{2v\phi}+\frac{M^2\phi_1}{4v\phi}\right\}$$
$$\times\left[\left(\frac{1-s_1}{1+s_1}\right)\left(\frac{1-s_2}{1+s_2}\right)\left(\frac{1-s_3}{1+s_3}\right)\right]^{m_f^2/4v}\frac{1}{(1-s_1^2)(1-s_2^2)(1-s_3^2)}$$
$$\times\frac{1}{\phi^2}\left[\lambda_1\frac{F_1}{\phi^2}+\lambda_2\left(\frac{F_2}{\phi^2}+m_f^2\frac{F_3}{\phi}+M^2\frac{F_4}{\phi^3}+k_1^2\frac{F_5}{\phi^3}+k_2^2\frac{F_6}{\phi^3}\right)+\lambda_3[(M^2+k_1^2+k_2^2)^2-4k_1^2k_2^2]\frac{F_7}{\phi^4}\right] \tag{C1}$$

in different regimes over momenta k_1^2 and k_2^2. Here and below dimensionless notations for momenta and masses like $M\equiv M/\Lambda$ are used. It is convenient to use the following representation for λ_i-functions (22)

$$\lambda_1(\rho)=\frac{1}{2}\int_{-1}^1 d\kappa\exp\kappa\rho,\qquad \lambda_2(\rho)=\frac{1}{4}\int_{-1}^1 d\kappa(\kappa^2-1)\exp\kappa\rho,\qquad \lambda_3(\rho)=\frac{1}{16}\int_{-1}^1 d\kappa(\kappa^2-1)^2\exp\kappa\rho,$$

in the integral (C1) in order to represent it as

$$I^{fn}(M^2,k_1^2,k_2^2)=\int_{-1}^1 d\kappa\int_0^1 ds_1\int_0^1 ds_2\int_0^1 ds_3\int_0^1 dt t^n\frac{\partial^n}{\partial t^n}$$
$$\times\exp\left\{-\frac{k_1^2\phi_{11}+k_2^2\phi_{12}}{2v\phi}+\frac{M^2\phi_1}{4v\phi}+\kappa\frac{\phi_2}{2v\phi}\sqrt{M^4+(k_1^2-k_2^2)^2+2M^2(k_1^2+k_2^2)}\right\} \tag{C2}$$
$$\times\left[\left(\frac{1-s_1}{1+s_1}\right)\left(\frac{1-s_2}{1+s_2}\right)\left(\frac{1-s_3}{1+s_3}\right)\right]^{m_f^2/4v}\frac{1}{(1-s_1^2)(1-s_2^2)(1-s_3^2)}$$
$$\times\frac{1}{\phi^2}\left[\frac{F_1}{2\phi^2}+\frac{1}{4}(\kappa^2-1)\left(\frac{F_2}{\phi^2}+m_f^2\frac{F_3}{\phi}+M^2\frac{F_4}{\phi^3}+k_1^2\frac{F_5}{\phi^3}+k_2^2\frac{F_6}{\phi^3}\right)\right.$$
$$\left.+\frac{1}{16}(\kappa^2-1)^2[(M^2+k_1^2+k_2^2)^2-4k_1^2k_2^2]\frac{F_7}{\phi^4}\right]. \tag{C3}$$

Below two different kinematic regimes are considered.

1. Asymmetric kinematics: $k_1=Q^2, k_2^2=0$

In this case the integral reads

$$I^{fn}(M^2,Q^2,0)=\int_{-1}^1 d\kappa\int_0^1 ds_1\int_0^1 ds_2\int_0^1 ds_3\int_0^1 dt t^n\frac{\partial^n}{\partial t^n}\exp\left\{-\frac{Q^2\phi_{11}}{2v\phi}+\frac{M^2\phi_1}{4v\phi}+\kappa\frac{\phi_2}{2v\phi}(M^2+Q^2)\right\}$$
$$\times\left[\left(\frac{1-s_1}{1+s_1}\right)\left(\frac{1-s_2}{1+s_2}\right)\left(\frac{1-s_3}{1+s_3}\right)\right]^{m_f^2/4v}\frac{1}{(1-s_1^2)(1-s_2^2)(1-s_3^2)}$$
$$\times\frac{1}{\phi^2}\left[\frac{1}{2}\frac{F_1}{\phi^2}+\frac{1}{4}(\kappa^2-1)\left(\frac{F_2}{\phi^2}+m_f^2\frac{F_3}{\phi}+M^2\frac{F_4}{\phi^3}+Q^2\frac{F_5}{\phi^3}\right)+\frac{1}{16}(\kappa^2-1)^2(M^2+Q^2)^2\frac{F_7}{\phi^4}\right]. \tag{C4}$$

For studying the large Q^2 limit, it is convenient to separate dependence on s_2 and define polynomials χ_i which depend on other integration variables,

$$\chi_1=s_1+tv+s_1s_3tv,\qquad \chi_2=s_1s_3+(s_1+s_3)tv,$$
$$\chi_3=2s_1s_3(1+s_2\kappa)+tv(s_1-s_2+s_3-s_1s_2s_3+2s_2\kappa(s_1+s_3)),$$

so that the expression in the exponent takes the form:

$$-\frac{Q^2\phi_{11}}{2v\phi}+\frac{M^2\phi_1}{4v\phi}+\kappa\frac{\phi_2}{2v\phi}(M^2+Q^2)$$
$$=-\frac{s_2(\chi_1-\kappa\chi_2)}{2v\phi}Q^2+\frac{\chi_3}{4v\phi}M^2.$$

One can see from the argument of the exponent in (C4) that the asymptotic behavior of the integral at large Q^2 is determined by the vicinity of $s_2=0$, which corresponds to the ultraviolet (short distance) regime in the translation invariant part quark propagator (15) between two photons; see Fig. 3. The leading short distance form of H_f is not modified by the background field, it simply corresponds to the standard free Euclidean quark propagator. However the translation noninvariant phase in full propagator (14) may mix up the short and large distance regimes in diagram 3 as a whole, thus leading to a modification of the asymptotic behavior of the form factor at large momenta.

Keeping only the lowest-order terms in the expansion of the integrand at $s_2=0$ one arrives at the asymptotics of the integral,

$$I^{fn}(-M^2,Q^2,0)\sim\mathcal{I}^{fn}_{\gamma^*\gamma}/Q^2,$$

with Q-independent coefficient

$$\mathcal{I}^{fn}_{\gamma^*\gamma}=\int_0^1 ds_1\int_0^1 ds_3\int_{-1}^1 d\kappa\int_0^1 dt t^n\frac{\partial^n}{\partial t^n}\left[\left(\frac{1-s_1}{1+s_1}\right)\left(\frac{1-s_3}{1+s_3}\right)\right]^{\frac{m_f^2}{4v}}\frac{1}{(1-s_1^2)(1-s_3^2)}\exp\left\{M^2\frac{\chi_3}{4v\phi}\right\}$$
$$\times\frac{2v}{(\chi_1-\kappa\chi_2)\phi}\left[\frac{1}{2}\frac{F_1}{\phi^2}+\frac{1}{4}(\kappa^2-1)\left(\frac{F_2}{\phi^2}+\frac{2v}{(\chi_1-\kappa\chi_2)\phi^2}\frac{\partial F_5}{\partial s_2}\right)+\frac{1}{16}(\kappa^2-1)^2\frac{4v^2}{(\chi_1-\kappa\chi_2)^2\phi^2}\frac{\partial^2F_7}{\partial s_2^2}\right]\Bigg|_{s_2=0}. \quad \text{(C5)}$$

The variable κ can be integrated out analytically:

$$\int_{-1}^1 d\kappa\frac{1}{\chi_1-\kappa\chi_2}=\frac{1}{\chi_2}\ln\frac{\chi_1+\chi_2}{\chi_1-\chi_2},$$
$$\int_{-1}^1 d\kappa\frac{\kappa^2-1}{\chi_1-\kappa\chi_2}=-2\frac{\chi_1}{\chi_2^2}+\frac{\chi_1^2}{\chi_2^3}\ln\frac{\chi_1+\chi_2}{\chi_1-\chi_2}-\frac{1}{\chi_2}\ln\frac{\chi_1+\chi_2}{\chi_1-\chi_2},$$
$$\int_{-1}^1 d\kappa\frac{\kappa^2-1}{(\chi_1-\kappa\chi_2)^2}=\frac{4}{\chi_2^2}-2\frac{\chi_1}{\chi_2^3}\ln\frac{\chi_1+\chi_2}{\chi_1-\chi_2},$$
$$\int_{-1}^1 d\kappa\frac{(\kappa^2-1)^2}{(\chi_1-\kappa\chi_2)^3}=-12\frac{\chi_1}{\chi_2^4}+6\frac{\chi_1^2}{\chi_2^5}\ln\frac{\chi_1+\chi_2}{\chi_1-\chi_2}-\frac{2}{\chi_2^3}\ln\frac{\chi_1+\chi_2}{\chi_1-\chi_2},$$
$$\frac{\chi_1+\chi_2}{\chi_1-\chi_2}=\frac{1+s_3}{1-s_3}\frac{s_1+tv+s_1tv}{s_1+tv-s_1tv}.$$

After substitution of this result to Eq. (C3), the rest of the integrals can be calculated numerically. The result contributes to coefficient $\varkappa_{\gamma^*\gamma}=1.23$ in Eq. (2).

If we now neglect the main effect of the background field by eliminating the term $\kappa\chi_2$ in Eq. (C5), then numerical calculation of the asymptotics gives the value $\varkappa_{\gamma^*\gamma}=1.014$ which agrees with the factorization limit very well.

2. Symmetric kinematics: $k_2^2=k_1^2=Q^2$

The integral takes the form

$$I^{fn}(M^2,Q^2,Q^2)=\int_{-1}^1 d\kappa\int_0^1 ds_1\int_0^1 ds_2\int_0^1 ds_3\int_0^1 dt t^n\frac{\partial^n}{\partial t^n}$$
$$\times\exp\left\{-\frac{\phi_{11}+\phi_{12}}{2v\phi}Q^2+\frac{\phi_1}{4v\phi}M^2+\kappa\frac{\phi_2}{2v\phi}\sqrt{M^4+4M^2Q^2}\right\}$$
$$\times\left[\left(\frac{1-s_1}{1+s_1}\right)\left(\frac{1-s_2}{1+s_2}\right)\left(\frac{1-s_3}{1+s_3}\right)\right]^{m_f^2/4v}\frac{1}{(1-s_1^2)(1-s_2^2)(1-s_3^2)}$$
$$\times\frac{1}{\phi^2}\left[\frac{1}{2}\frac{F_1}{\phi^2}+\frac{1}{4}(\kappa^2-1)\left(\frac{F_2}{\phi^2}+m_f^2\frac{F_3}{\phi}+M^2\frac{F_4}{\phi^3}+Q^2\frac{F_5+F_6}{\phi^3}\right)+\frac{1}{16}(\kappa^2-1)^2(M^4+4M^2Q^2)\frac{F_7}{\phi^4}\right]. \quad \text{(C6)}$$

For $Q^2 \gg M^2$ the second term in the exponent in Eq. (C6) is subleading with respect to ϕ_1 [see (C7)] as it is linear in $|Q|$. In other words, term (19) does not contribute to the asymptotic behavior of the form factor in symmetric kinematics, that is the crucial difference between asymmetric and symmetric kinematic regimes.

$$\mathcal{I}^{fn}_{\gamma^*\gamma^*} = 2v\int_0^1 ds_1\int_0^1 ds_3\int_0^1 dt t^n \frac{\partial^n}{\partial t^n}\left[\left(\frac{1-s_1}{1+s_1}\right)\left(\frac{1-s_3}{1+s_3}\right)\right]^{\frac{m_f^2}{4v}}\frac{1}{(1-s_1^2)(1-s_3^2)} \times\frac{1}{\phi^4}\left[F_1-\frac{1}{3}F_2\right]\exp\left\{M^2\frac{\phi_1}{4v\phi}\right\}\Big|_{s_2=0}.$$

Taking into account the explicit form of the polynomials F_1, F_2, ϕ, and ϕ_1 at $s_2=0$ one arrives at

$$\mathcal{I}^{fn}_{\gamma^*\gamma^*} = 8v\int_0^1 ds_1\int_0^1 ds_3\int_0^1 dt t^n \frac{\partial^n}{\partial t^n}\left[\left(\frac{1-s_1}{1+s_1}\right)\left(\frac{1-s_3}{1+s_3}\right)\right]^{\frac{m_f^2}{4v}}\frac{1}{(1-s_1^2)(1-s_3^2)} \times\frac{(1+s_1s_3)[(1-s_1s_3)(s_1+s_3)+2vt(1-s_1^2)(1-s_3^2)]}{(s_1+s_3+2vt(1+s_1s_3))^3}\times\exp\left\{M^2\frac{2s_1s_3+vt(s_1+s_3)}{4v(s_1+s_3+2vt(1+s_1s_3))}\right\}. \tag{C7}$$

Substituting this expression into (17), one obtains for the form factor of the ath component of the flavor pseudoscalar multiplet with radial excitation number n

$$Q^2F_{P_{an}\gamma^*\gamma^*}(Q^2)\sim\Lambda\frac{h_{aP0n}}{16\pi^2}\sum_{n',f,v}\frac{1}{v}\mathcal{O}^{ab}_{nn'}\mathcal{M}^b_{ff}q_f^2m_f\mathcal{I}^{fn'}_{\gamma^*\gamma^*}. \tag{C8}$$

In particular, for the π-meson which corresponds to $a=3$ and $n=0$ one arrives at

$$Q^2F_{\pi\gamma^*\gamma^*}(Q^2)\sim\frac{\sqrt{2}}{3}f_\pi \tag{C9}$$

with the constant

$$f_\pi = m\frac{h_\pi}{4\pi^2}\sum_{n,v}\mathcal{O}^{33}_{0n}\int_0^1 ds_1\int_0^1 ds_3\int_0^1 dt t^n\frac{\partial^n}{\partial t^n}\left[\left(\frac{1-s_1}{1+s_1}\right)\left(\frac{1-s_3}{1+s_3}\right)\right]^{\frac{m^2}{4v\Lambda^2}}\frac{1}{(1-s_1^2)(1-s_3^2)} \times\frac{(1+s_1s_3)[(1-s_1s_3)(s_1+s_3)+2vt(1-s_1^2)(1-s_3^2)]}{(s_1+s_3+2vt(1+s_1s_3))^3}\times\exp\left\{\frac{M^2}{4v\Lambda^2}\frac{2s_1s_3+vt(s_1+s_3)}{(s_1+s_3+2vt(1+s_1s_3))}\right\}, \tag{C10}$$

where we have restored dimension of the light quark and π-meson masses, m and M, respectively. Constant f_π defined by Eq. (C10) exactly coincides with the contribution of the diagram (a) in Fig. 9 to the charged pion weak decay constant, as it can be seen from Eq. (27) in paper [37]. The contribution of the second diagram (b) typical for all nonlocal approaches to the quark-meson vertices does not appear in the large Q^2 limit of the pion transition form factor.

APPENDIX D: DIAGRAMS INCLUDING NONLOCAL MESON-PHOTON VERTICES

This appendix is devoted to the calculation of diagrams C and D shown in Fig. 3. The nonlocal vertex describing meson-photon interaction (see [37] for details) is defined as

$$V^{aJln}_{A_\mu(k)}(x) = \int_0^1 d\tau\frac{1}{\tau}\frac{\partial}{\partial k_\mu}\{e_fV^{aJln}(\overleftrightarrow{\mathcal{D}}(x)+ik\tau\xi)-e_{f'}V^{aJln}(\overleftrightarrow{\mathcal{D}}(x)-ik\tau\xi')\}, \tag{D1}$$

where k is the momentum of the photon, and $V^{aJln}(\overleftrightarrow{\mathcal{D}}(x))$ is given by Eq. (13). In particular, the vertex for neutral pseudoscalar unflavored mesons and pseudoscalar quarkonia is

$$V^{aP0n}_{A_\mu(k)}(x) = i\gamma_5\mathcal{C}_{0n}\sum_f\mathcal{M}^a_{ff}e_f\int_0^1\frac{d\tau}{\tau}\left\{\frac{\partial}{\partial k_\mu}F_{n0}\left(\left(\overleftrightarrow{\mathcal{D}}(x)+\frac{i}{2}k\tau\right)^2\right)+(k\to-k)\right\},$$

where dimensionless notation is used. The contribution of diagram C in Fig. 3 in momentum representation is given by

$$C^{an}_{\mu\nu}(p,k_1,k_2) = h_{aP0n}\sum_{n',f}\mathcal{O}^{ab}_{nn'}\mathcal{C}_{0n'}\mathcal{M}^a_{ff}e_f^2\int dx e^{i(p-k_1)x}\int dy e^{-ik_2y}$$
$$\times\int d\sigma_B\left[\int_0^1 d\tau\frac{1}{\tau}\frac{\partial}{\partial k_{2\mu}}\mathrm{Tr}i\gamma_5 F_{n0}\left(\left(\overleftrightarrow{\mathcal{D}}(x)+\frac{i}{2}k_2\tau\right)^2\right)S_f(x,y)\gamma_\mu S_f(y,x)+(k_2\to -k_2)\right]$$
$$=\pm(2\pi)^4\delta^{(4)}(p-k_1-k_2)h_{aP0n}\sum_{n',f}\mathcal{O}^{ab}_{nn'}\mathcal{C}_{0n'}\mathcal{M}^a_{ff}e_f^2\int d\sigma_B\left[\int_0^1 ds_1\int_0^1 ds_2\int_0^1 d\tau\int_0^1 dt t^{n'}\frac{\partial^{n'}}{\partial t^{n'}}\right.$$
$$\times\left(\frac{1-s_1}{1+s_1}\right)^{\frac{m_f}{4v}}\left(\frac{1-s_2}{1+s_2}\right)^{\frac{m_f}{4v}}\exp\{if_{\rho\eta}k_{1\rho}k_{2\eta}\phi_1+\phi_2k_1^2+\phi_3k_1k_2+\phi_4k_2^2\}(F_1\delta_{\mu\nu}+F_2k_{1\mu}k_{1\nu}+F_3k_{1\mu}k_{2\nu}$$
$$+F_4k_{1\nu}k_{2\mu}+F_5k_{2\mu}k_{2\nu}+F_6f_{\alpha\mu}k_{1\alpha}k_{1\nu}+F_7f_{\alpha\mu}k_{1\alpha}k_{2\nu}+F_8f_{\alpha\nu}k_{1\alpha}k_{1\mu}+F_9f_{\alpha\nu}k_{1\alpha}k_{2\mu}+F_{10}f_{\alpha\nu}k_{2\alpha}k_{1\mu}$$
$$\left.+F_{11}f_{\alpha\nu}k_{2\alpha}k_{2\mu}+F_{12}f_{\alpha\mu}f_{\beta\nu}k_{1\alpha}k_{1\beta}+F_{13}f_{\alpha\mu}f_{\beta\nu}k_{1\alpha}k_{2\beta}+F_{14}f_{\mu\nu})+(k_2\to -k_2)\right]. \quad \text{(D2)}$$

Here $\pm$ stays for "+" in the case of the self-dual field and "−" otherwise, and functions ϕ_i and F_i are rational functions of integration variables s_1, s_2, t, τ. Integration over the background field is given by formulas

$$\langle\exp(if_{\mu\nu}J_{\mu\nu})\rangle=\frac{\sin\sqrt{2(J_{\mu\nu}J_{\mu\nu}\pm J_{\mu\nu}\tilde{J}_{\mu\nu})}}{\sqrt{2(J_{\mu\nu}J_{\mu\nu}\pm J_{\mu\nu}\tilde{J}_{\mu\nu})}},$$
$$\langle f_{\alpha\beta}\exp(if_{\mu\nu}J_{\mu\nu})\rangle=\frac{1}{2i}\frac{\partial}{\partial J_{\alpha\beta}}\langle\exp(if_{\mu\nu}J_{\mu\nu})\rangle,\ \langle f_{\rho\eta}f_{\alpha\beta}\exp(if_{\mu\nu}J_{\mu\nu})\rangle=\frac{1}{(2i)^2}\frac{\partial}{\partial J_{\rho\eta}}\frac{\partial}{\partial J_{\alpha\beta}}\langle\exp(if_{\mu\nu}J_{\mu\nu})\rangle,$$

and averaging over self-dual and anti-self-dual configurations. Here $J_{\mu\nu}$ is an antisymmetric tensor. For (D2) the tensor is

$$J_{\mu\nu}=\frac{1}{2}(k_{1\mu}k_{2\nu}-k_{1\nu}k_{2\mu})\phi_1.$$

The result of integration of $C^{an}_{\mu\nu}$ over $d\sigma_B$ is exactly zero.

To consider diagram D in Fig. 3 one needs the vertex for neutral pseudoscalar unflavored mesons and pseudoscalar quarkonia with two photons given by

$$V^{aP0n}_{A_\mu(k)A_\nu(q)}(x)=i\gamma_5\mathcal{C}_{0n}\sum_f\mathcal{M}^a_{ff}e_f\int_0^1\frac{d\tau_1}{\tau_1}\int_0^1\frac{d\tau_2}{\tau_2}\left\{\frac{\partial}{\partial k_\mu}\frac{\partial}{\partial q_\nu}F_{n0}\left(\left(\overleftrightarrow{\mathcal{D}}(x)+\frac{i}{2}k\tau_1+\frac{i}{2}q\tau_2\right)^2\right)\right.$$
$$\left.+(k\to -k)+(q\to -q)+(k\to -k,q\to -q)\right\}.$$

The contribution of diagram D in momentum representation is given by

$$D^{an}_{\mu\nu}(p,k_1,k_2)=h_{aP0n}\sum_{n',f}\mathcal{O}^{ab}_{nn'}\mathcal{C}_{0n'}\mathcal{M}^a_{ff}e_f^2\int dx e^{i(p-k_1-k_2)x}\int_0^1\frac{d\tau_1}{\tau_1}\int_0^1\frac{d\tau_2}{\tau_2}\int d\sigma_B$$
$$\times\left[\frac{\partial}{\partial k_{1\mu}}\frac{\partial}{\partial k_{2\nu}}\mathrm{Tr}i\gamma_5F_{n0}\left(\left(\overleftrightarrow{\mathcal{D}}(x)+\frac{i}{2}k_1\tau_1+\frac{i}{2}k_2\tau_2\right)^2\right)S_f(x,x)\right.$$
$$\left.+(k_1\to -k_1)+(k_2\to -k_2)+(k_1\to -k_1,k_2\to -k_2)\right]$$
$$=\pm(2\pi)^4\delta^{(4)}(p-k_1-k_2)h_{aP0n}\sum_{n',f}\mathcal{O}^{ab}_{nn'}\mathcal{C}_{0n'}\mathcal{M}^a_{ff}e_f^2\int_0^1 d\tau_1\int_0^1 d\tau_2\int d\sigma_B\left[\int_0^1 ds\int_0^1 dt t^{n'}\frac{\partial^{n'}}{\partial t^{n'}}\right.$$
$$\times\left(\frac{1-s}{1+s}\right)^{\frac{m_f}{4v}}F_{15}\left(\frac{\partial}{\partial k_{1\mu}}\frac{\partial}{\partial k_{2\nu}}\exp\{\phi_5k_1^2+\phi_6k_1k_2+\phi_7k_2^2\}+(k_1\to -k_1)\right.$$
$$\left.\left.+(k_2\to -k_2)+(k_1\to -k_1,k_2\to -k_2)\right)\right].$$

Here ϕ_i, F_i are rational functions in s,t,τ_1,τ_2. Integration over $d\sigma_B$ yields zero.

[1] B. Aubert *et al.* (*BABAR* Collaboration), Phys. Rev. D **80**, 052002 (2009).
[2] G. P. Lepage and S. J. Brodsky, Phys. Rev. D **22**, 2157 (1980).
[3] S. Uehara *et al.* (Belle Collaboration), Phys. Rev. D **86**, 092007 (2012).
[4] S. V. Mikhailov and N. G. Stefanis, Nucl. Phys. **B821**, 291 (2009).
[5] S. S. Agaev, V. M. Braun, N. Offen, and F. A. Porkert, Phys. Rev. D **83**, 054020 (2011).
[6] A. P. Bakulev, S. V. Mikhailov, A. V. Pimikov, and N. G. Stefanis, Phys. Rev. D **86**, 031501 (2012).
[7] Y. Klopot, A. Oganesian, and O. Teryaev, Phys. Rev. D **87**, 036013 (2013); **88**, 059902(E) (2013).
[8] A. G. Oganesian, A. V. Pimikov, N. G. Stefanis, and O. V. Teryaev, Phys. Rev. D **93**, 054040 (2016).
[9] W. Lucha and D. Melikhov, J. Phys. G **39**, 045003 (2012).
[10] H. n. Li and S. Mishima, Phys. Rev. D **80**, 074024 (2009).
[11] P. Kroll, Eur. Phys. J. C **71**, 1623 (2011).
[12] M. Gorchtein, P. Guo, and A. P. Szczepaniak, Phys. Rev. C **86**, 015205 (2012).
[13] F. Zuo, Y. Jia, and T. Huang, Eur. Phys. J. C **67**, 253 (2010).
[14] A. Stoffers and I. Zahed, Phys. Rev. C **84**, 025202 (2011).
[15] R. Swarnkar and D. Chakrabarti, Phys. Rev. D **92**, 074023 (2015).
[16] S. J. Brodsky, F. G. Cao, and G. F. de Teramond, Phys. Rev. D **84**, 033001 (2011).
[17] H. L. L. Roberts, C. D. Roberts, A. Bashir, L. X. Gutierrez-Guerrero, and P. C. Tandy, Phys. Rev. C **82**, 065202 (2010).
[18] A. E. Dorokhov, arXiv:1003.4693.
[19] A. E. Dorokhov, JETP Lett. **92**, 707 (2010).
[20] A. E. Dorokhov and E. A. Kuraev, Phys. Rev. D **88**, 014038 (2013).
[21] P. Kotko and M. Praszalowicz, Phys. Rev. D **81**, 034019 (2010).
[22] C. C. Lih and C. Q. Geng, Phys. Rev. C **85**, 018201 (2012).
[23] P. Lichard, Phys. Rev. D **83**, 037503 (2011).
[24] E. Ruiz Arriola and W. Broniowski, Phys. Rev. D **81**, 094021 (2010).
[25] H. Czyz, S. Ivashyn, A. Korchin, and O. Shekhovtsova, Phys. Rev. D **85**, 094010 (2012).
[26] N. I. Kochelev and V. Vento, Phys. Rev. D **81**, 034009 (2010).
[27] D. McKeen, M. Pospelov, and J. M. Roney, Phys. Rev. D **85**, 053002 (2012).
[28] T. N. Pham and X. Y. Pham, Int. J. Mod. Phys. A **26**, 4125 (2011).
[29] A. E. Dorokhov, Phys. Part. Nucl. Lett. **7**, 229 (2010).
[30] A. V. Radyushkin, Phys. Rev. D **80**, 094009 (2009).
[31] M. V. Polyakov, JETP Lett. **90**, 228 (2009).
[32] G. V. Efimov and S. N. Nedelko, Phys. Rev. D **51**, 176 (1995).
[33] J. V. Burdanov, G. V. Efimov, S. N. Nedelko, and S. A. Solunin, Phys. Rev. D **54**, 4483 (1996).
[34] A. C. Kalloniatis and S. N. Nedelko, Phys. Rev. D **64**, 114025 (2001);
[35] A. C. Kalloniatis and S. N. Nedelko, Phys. Rev. D **69**, 074029 (2004).
[36] S. N. Nedelko and V. E. Voronin, Eur. Phys. J. A **51**, 45 (2015).
[37] S. N. Nedelko and V. E. Voronin, Phys. Rev. D **93**, 094010 (2016).
[38] S. N. Nedelko and V. E. Voronin, Int. J. Mod. Phys. Conf. Ser. **39**, 1560105 (2015).
[39] A. V. Radyushkin and R. T. Ruskov, Nucl. Phys. **B481**, 625 (1996).
[40] V. Bernard, A. H. Blin, B. Hiller, U. G. Meissner, and M. C. Ruivo, Phys. Lett. B **305**, 163 (1993).
[41] H. B. Deng, X. L. Chen, and W. Z. Deng, Chin. Phys. C **38**, 013103 (2014).
[42] K. A. Olive *et al.* (Particle Data Group Collaboration), Chin. Phys. C **38**, 090001 (2014).
[43] T. W. Chiu *et al.* (TWQCD Collaboration), Phys. Lett. B **651**, 171 (2007).
[44] A. C. Kalloniatis and S. N. Nedelko, Phys. Rev. D **66**, 074020 (2002).
[45] H. J. Behrend *et al.* (CELLO Collaboration), Z. Phys. C **49**, 401 (1991).
[46] J. Gronberg *et al.* (CLEO Collaboration), Phys. Rev. D **57**, 33 (1998).
[47] P. del Amo Sanchez *et al.* (*BABAR* Collaboration), Phys. Rev. D **84**, 052001 (2011).
[48] J. P. Lees *et al.* (*BABAR* Collaboration), Phys. Rev. D **81**, 052010 (2010).